Received: 19 December 2025 | Revised: 8 April 2026 | Accepted: 12 May 2026

DOI: 10.1002/dvdy.70156

Developmental Dynamics | American Association for Anatomy | WILEY

PHENOTYPE REPORT

Spatial and temporal coordination of signaling pathways in tissue differentiation: Developmental atlas of protein expression during zebra finch beak maturation

Renée A. Duckworth[1] | **Sarah E. Britton**[1,2] | **Cody A. Lee**[1,3] | **Kathryn C. Chenard**[1,4] | **Alexander V. Badyaev**[1]

[1]Department of Ecology and Evolutionary Biology, University of Arizona, Tucson, Arizona, USA

[2]Department of Ecology, Behavior and Evolution, University of California San Diego, La Jolla, California, USA

[3]School of Medicine, University of California San Diego, La Jolla, California, USA

[4]Department of Integrative Biology, University of Texas at Austin, Austin, Texas, USA

Correspondence
Renée A. Duckworth, Department of Ecology and Evolutionary Biology, University of Arizona, Tucson, AZ, USA.
Email: rad3@arizona.edu

Funding information
National Science Foundation, Grant/Award Numbers: IBN-0218313, DEB-1754465

Abstract

Background: Morphogenesis depends on spatial and temporal coordination of signaling pathways, yet context-specificity in interactions among these pathways during cartilage and bone differentiation remains poorly understood. Here we map cellular and histological localization of regulatory proteins forming core craniofacial developmental pathways of the zebra finch (*Taeniopygia guttata*) to provide insight into their functional roles during beak morphogenesis.

Results: We present an atlas of spatiotemporal coexpression of β-catenin, Bmp4, CaM, Dkk3, Fgf8, Ihh, Tgfβ2, and Wnt4 across embryonic stages HH29–42. Early stages (HH29–32), showed broad expression across epithelial and mesenchymal tissues, followed by progressive compartmentalization by HH36, with pronounced divergence among tissues. Notably, at later stages, proteins showed tissue-specific distributions in boundary versus core regions of chondrogenic and osteogenic domains, indicating coordinated cross-pathway patterning during cartilage and bone formation.

Conclusions: We find that osteogenesis in the zebra finch beak is organized by coordinated signaling between boundary-associated cells and differentiating cores; cross-pathway feedback establishes bone and cartilage differentiation while maintaining boundaries. Our results corroborate core aspects of craniofacial signaling dynamics and yet reveal unexpected subcellular localization of some key proteins identifying regulatory complexity not captured by prior transcript-level maps. This atlas provides a protein-level baseline for comparative and mechanistic studies of avian beak morphogenesis.

KEYWORDS
chondrogenesis, craniofacial development, immunohistochemistry, mesenchymal stem cells, osteogenesis

1 | INTRODUCTION

During craniofacial development, signaling proteins exhibit dynamic expression patterns that integrate positional information and coordinate tissue differentiation.[1–4] The functions of these signals ultimately require their physical assembly, necessitating subcellular and within-tissue colocalization. In particular, distinguishing

between membranal, cytoplasmic, and nuclear compartmentalization of protein complexes is crucial for understanding pathway activation states and the directionality of communication at the tissue level.[5] For example, nuclear localization of transcriptional regulators could indicate active signaling, whereas cytoplasmic

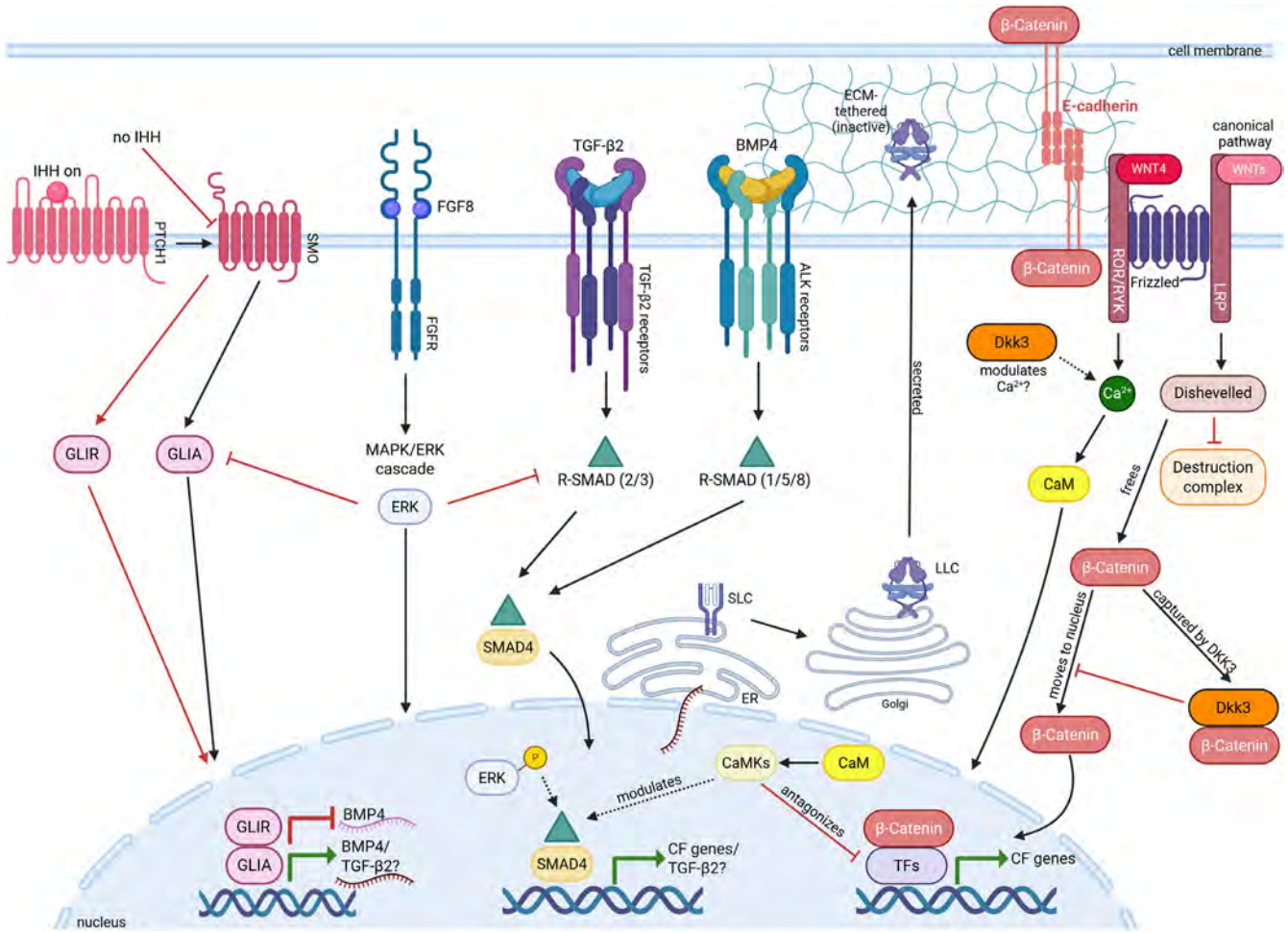

FIGURE 1 Summary of known and potential interactions of eight focal proteins in craniofacial development. HH signaling (far left) is initiated when IHH binds to cell surface receptor Patched 1 (PTCH1), activating Smoothened (SMO) which, in turn, initiates a signaling cascade activating Gli activator proteins (GLIA) which are key transcription factors for craniofacial (CF) genes, including BMP4 and TGFβ2. In the absence of IHH ligand, SMO is blocked and the Gli repressor (GLIR) is produced, blocking gene expression. BMP4 and TGFβ2 each initiate signaling cascades involving different sets of R-SMAD proteins that form a complex with SMAD4. This complex translocates to the nucleus where it recruits other co-activators or repressors (not shown) and binds DNA to activate (and sometimes repress) target CF genes, including in some cases TGFβ2. FGF8 signaling can block IHH, TGFβ2, and BMP4 pathways as it activates the MAPK/ERK pathway, and ERK can inhibit both GLIA and R-SMADs from reaching the nucleus. However, in some developmental contexts, ERK can enhance gene transcription or shift it to new target genes by phosphorylating R-SMADs in the nucleus. Unlike the other secreted ligands, TGFβ2 is translated as a pro-peptide that dimerizes in the endoplasmic reticulum (ER) and forms the small latent complex (SLC), which then binds latent TGFβ-binding protein in the Golgi to form the large latent complex (LLC). The LLC is secreted and tethered to the ECM in an inactive state until mechanically or proteolytically activated. WNT4 (far right) mainly acts as a non-canonical Wnt ligand by binding to a Frizzled/ROR- or Frizzled/RYK-type receptor complex to activate Ca^{2+} signaling, which elevates intracellular Ca^{2+} and activates calmodulin (CaM) and downstream kinases (CamKs) either in the cytoplasm (not shown) or the nucleus. These kinases, in turn, provide context-dependent modulation of Smads and other CF-relevant transcription factors (TF). In parallel, a separate canonical Wnt pathway activates the LRP-Frizzled-Disheveled axis, blocking the destruction complex and stabilizing cytoplasmic β-catenin. This enables its nuclear translocation to regulate craniofacial (CF) genes with TCF/LEF (T cell factor/lymphoid enhancer factor family; not shown) and other transcription factors. Non-canonical WNT4/Ca^{2+}/CaM signaling can antagonize canonical output by inhibiting TCF/β-catenin-dependent transcriptional activity. Dkk3 is a context-dependent modulator of this axis, as it has been proposed to modulate Ca^{2+} production, although the mechanism is still under investigation. DKK3 can also capture cytoplasmic β-catenin, limiting its nuclear entry and further impacting canonical Wnt activity. In the absence of canonical Wnt signaling, a pool of β-catenin is bound to E-cadherin at adherens junctions in the cell membrane, contributing to cell–cell adhesion and sequestering β-catenin away from the nucleus.

localization suggests ligand production or initiation of intracellular signaling cascades.[6–8] Thus, by placing subcellular localizations in a spatial and temporal context, we can gain insight into the flow and distribution of information among cells as well as the functional importance of expression overlap for tissue differentiation.

While prior work has focused mainly on transcript-level expression maps,[9] in this study, we trace ontogenetic changes in the colocalization and compartmentalization of regulatory proteins across multiple signaling pathways important in avian beak development. Maps of protein localization are a powerful complementary approach to transcript-level maps because they are often a closer proxy for the stage-specific functional performance of signaling pathways.[10] Because turnover rates of transcripts and proteins often differ[11,12] and spatial context is important for interpreting the functional significance of

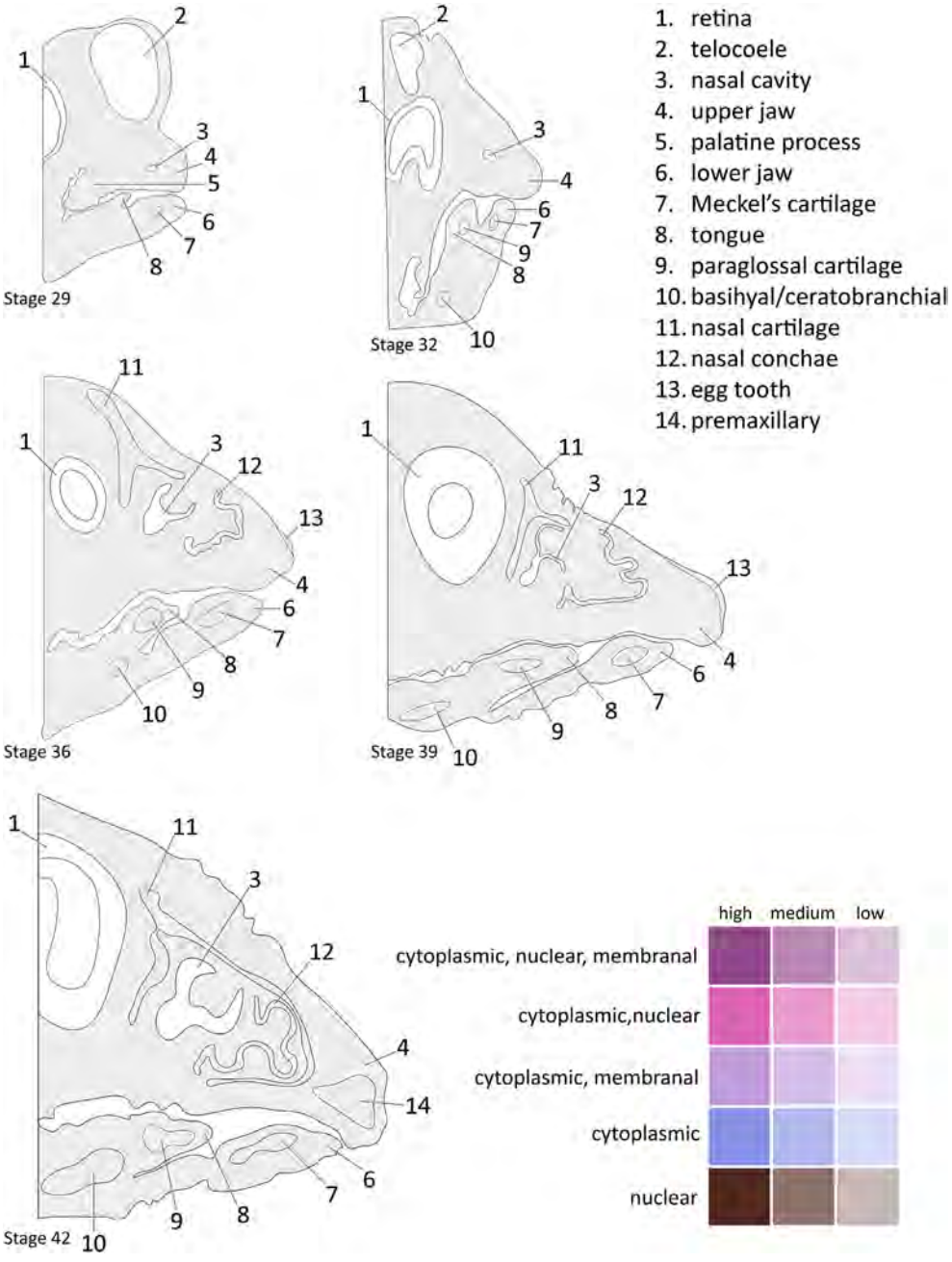

FIGURE 2 Consensus illustrations of mid-sagittal sections of five developmental stages traced from prototypical embryos used in this study with major anatomical features labeled. Key shows color scheme used to denote cellular localization of expression as well as expression intensity in Figures 3–12. Nuclear expression includes perinuclear.

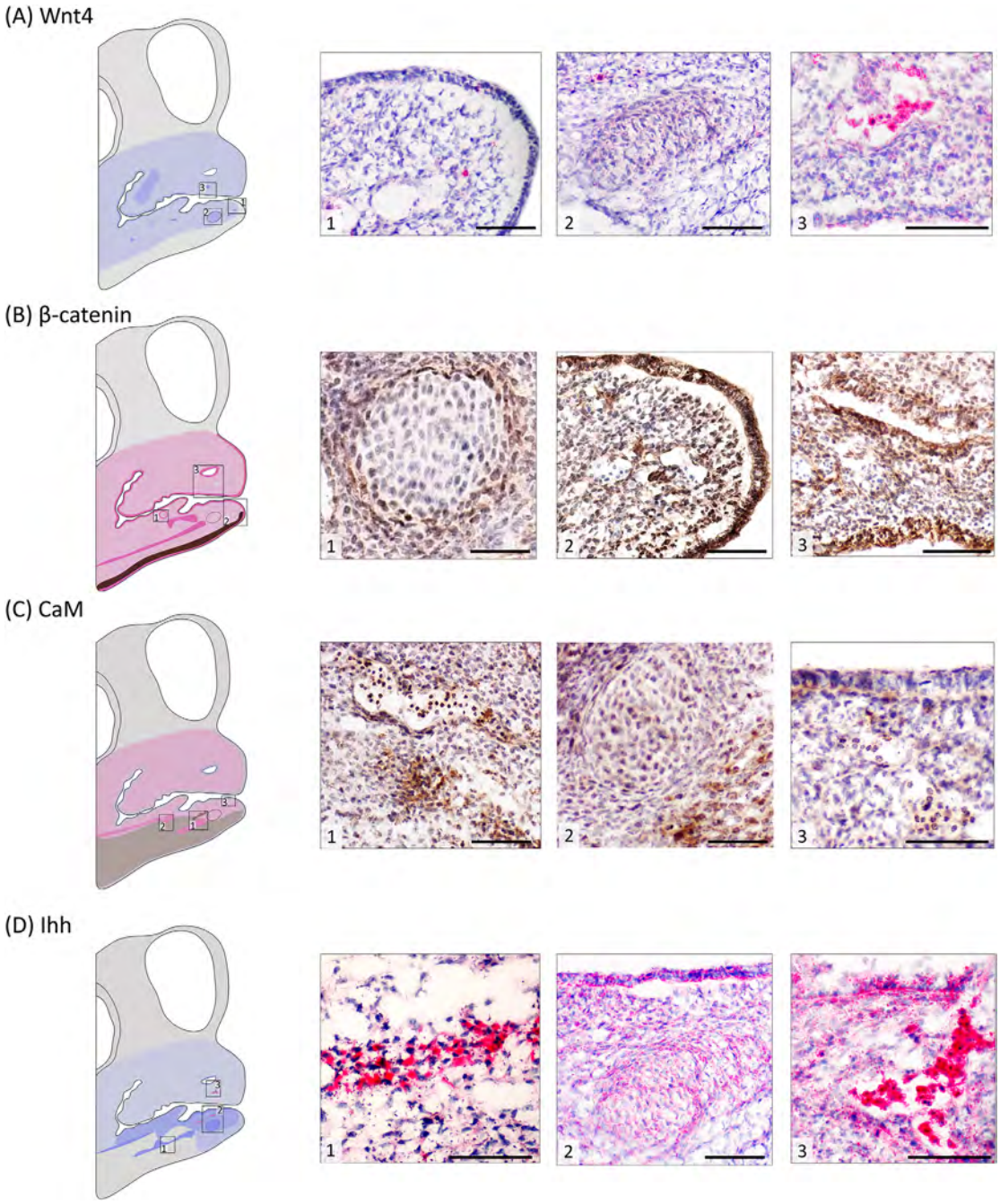

FIGURE 3 Wnt4, *β*-catenin, CaM, and Ihh expression at stage HH29/30. (A) Wnt4 (red stain) shows weak cytoplasmic expression overall with (1) no expression at the tip and ventral portion of the mandibular prominence and (2) weak to moderate expression in the Meckel's condensation. (3) Strong cytoplasmic and perinuclear expression in blood cells. (B) *β*-catenin expression (second panel, brown stain) is widespread in both upper and lower jaw with (1) the weakest expression in pre-cartilage condensations (paraglossal shown) which are surrounded by cells showing strong nuclear expression. (2) Nuclear and cytoplasmic expression in the surface epithelium of both the upper and lower jaw (lower mandibular tip shown) with expression limited to nuclear in the ventral portion of the mandibular prominence. (3) Strong nuclear and cytoplasmic expression in the nasal and oral epithelium of the maxillary prominence. (C) CaM (brown stain) shows moderate nuclear and cytoplasmic expression in both the maxilla and mandible with (1, 2) stronger expression in potentially myogenic areas adjacent to pre-cartilage condensations. Strong nuclear expression in blood cells. (3) Epithelial expression is cytoplasmic with scattered nuclear expression in the underlying mesenchyme. (D) Ihh (red stain) shows overall weak expression in the maxillary prominence, and is stronger, albeit more localized to specific regions, in the mandibular prominence. (1) There is a stripe of strong cytoplasmic expression in likely pre-myogenic tissue along the center of the mandibular prominence and (2) moderate expression in the oral epithelium that matches underlying expression in the Meckel's condensation. (3) Strong cytoplasmic expression in blood cells and at the edge of the nasal cavity. See Figure 2 for key to anatomical features and expression patterns. Photos here and throughout 40×. Scale bars: 50 μm.

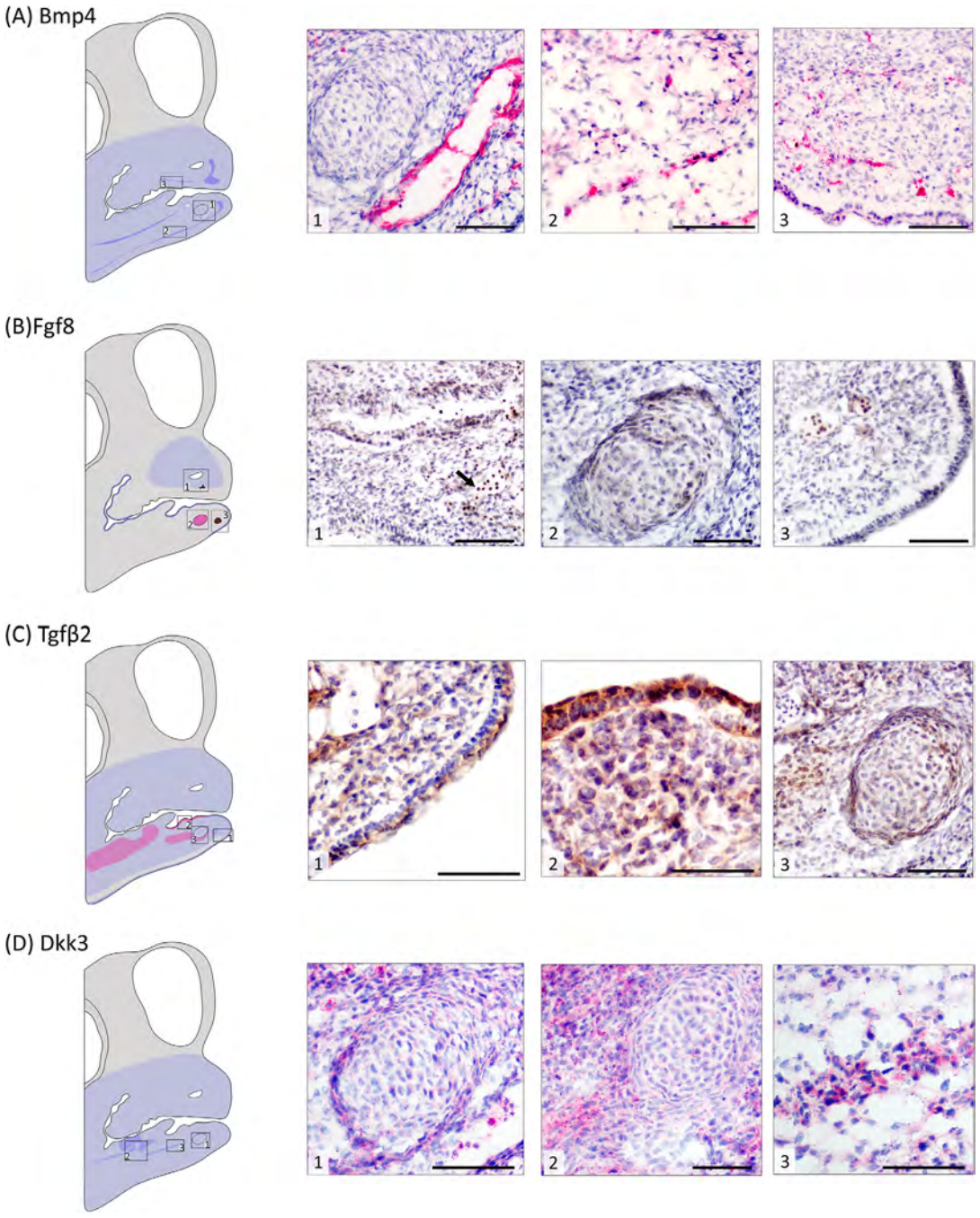

FIGURE 4 Bmp4, Fgf8, TGF-β, and Dkk3 expression at stage HH29/30. (A) Bmp4 (red stain) shows relatively weak cytoplasmic expression overall with (1) with strong expression concentrated around blood vessels and in stripes of mesenchymal tissue in both the (2) lower and (3) upper ventral beak margins. Spatial extent of (B) Fgf8 expression (brown stain) is limited in the upper and lower jaw. (1) Maxillary prominence shows weak cytoplasmic expression around the nasal cavity with strong nuclear expression only in blood cells (arrow). (2) Meckel's cartilage shows weak cytoplasmic expression with areas of strong perinuclear expression, especially at the periphery. (3) Weak cytoplasmic expression in the mesenchyme and surface epithelium. (C) TGF-β2 (brown stain) shows relatively weak cytoplasmic expression in the upper and lower beak prominences. (1) Weak cytoplasmic expression in mesenchyme shifts to moderately strong around developing vascular opening and moderately strong staining in surface epithelium of the mandibular prominence. (2) Strong cytoplasmic and perinuclear staining in the oral epithelium of the lower beak prominence. Meckel's condensation shows weak cytoplasmic staining with moderate perinuclear expression in the perichondrogenic area and in an adjacent pre-myogenic area. (D) Dkk3 (red stain) shows weak cytoplasmic expression in both prominences with regions of stronger expression in the mandibular prominence. (1) Elevated perichondrogenic expression for the Meckel's condensation and moderate expression in blood cells. (2) Moderate expression in the mesenchyme surrounding the basihyal condensation with only weak expression in the condensation itself. (3) Moderate expression in a stripe of mesenchymal tissue in the ventral margin of the mandibular process. See Figure 2 for key to anatomical features and expression patterns. Scale bars: 50 μm.

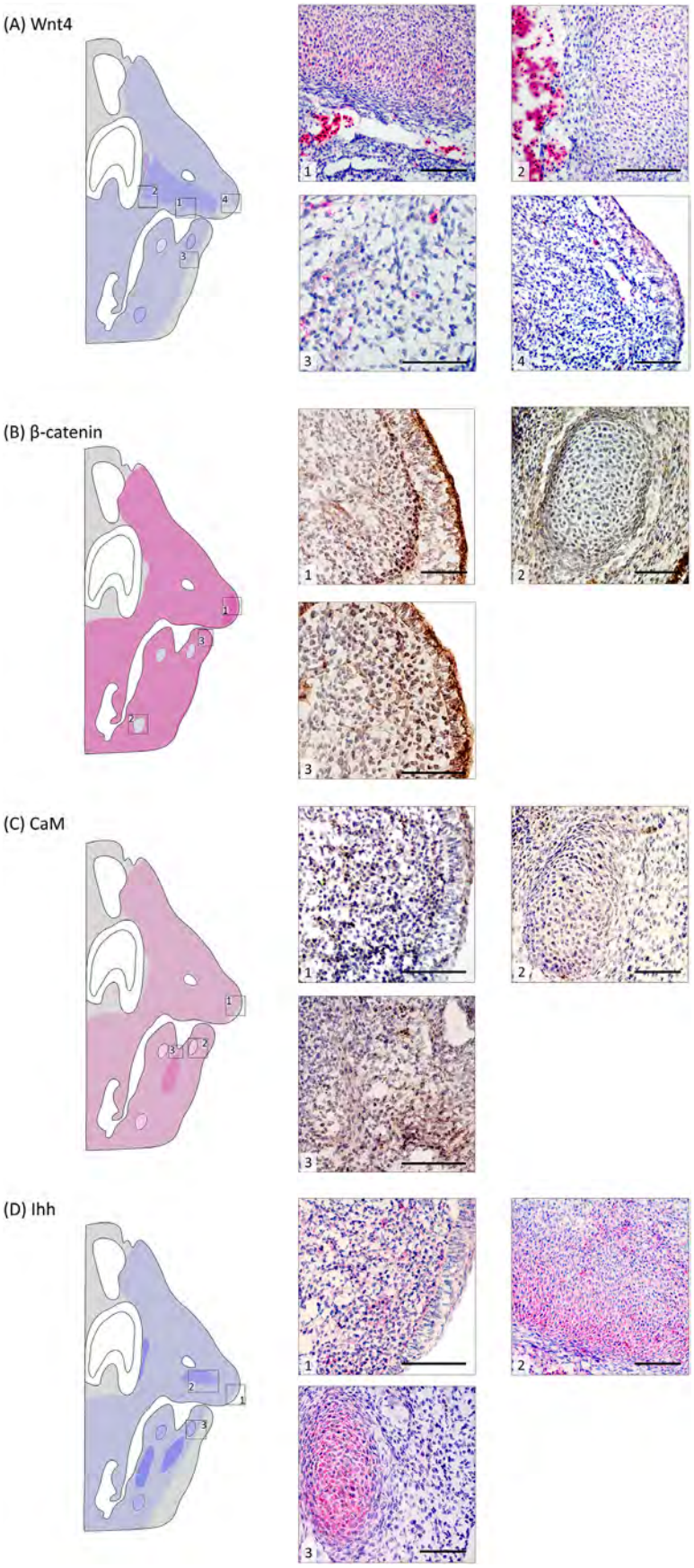

FIGURE 5 Legend on next page.

expression patterns,[13] a protein-level atlas that is coupled with detailed histological mapping can provide novel insight into coordinated signaling at boundaries and tissue interfaces. Comparing such detailed functional maps with prior work on gene expression can pinpoint where these maps diverge, which would, in turn, suggest novel regulation patterns and pathways for evolutionary change.[10] Here, we specifically focus on the temporal activation and spatial modulation of chondro- and osteogenic protein networks that play a key role in beak morphogenesis and evolution.

The development of the avian beak is a model for studies of evolutionary divergence in vertebrates and exploration of craniofacial abnormalities in humans.[14,15] This importance stems from a shared developmental architecture governed by four evolutionarily conserved signaling pathways: wingless type protein (Wnt), bone morphogenetic protein (Bmp; part of the transcription growth factor, Tgfβ, superfamily), fibroblast growth factor (Fgf), and hedgehog (Hh) signaling.[16–20] Here, we examine the cellular localization, developmental timing, and tissue-specific expression of eight key regulatory proteins from these pathways that have been well characterized in early stages of avian beak development[21–27]: β-catenin, bone morphogenic protein 4 (Bmp4), calmodulin (CaM), dickkopf homolog 3 (Dkk3), fibroblast growth factor 8 (Fgf8), Indian hedgehog (Ihh), transforming growth factor beta 2 (Tgfβ2), and wingless type 4 (Wnt4).

Wnt signaling regulates cell polarity, proliferation, and fate specification and interacts extensively with the other pathways integrating signals that orchestrate tissue patterning[28] (Figure 1). β-catenin and Wnt4 capture canonical and non-canonical components of the Wnt pathway,[24,29] respectively, while Dkk3 serves as a context-dependent Wnt modulator[30,31] (Figure 1). Bmp4 and Tgfβ2, both members of the TGF-β superfamily, represent key regulators of mesenchymal differentiation and epithelial–mesenchymal signaling.[32–34] FGF signaling, via four receptor subtypes, fine-tunes growth and differentiation of skeletal progenitors through feedback loops that ensure spatial and temporal precision.[35–39] Hh signaling, primarily through Sonic and Indian Hedgehog (Shh and Ihh, respectively), maintains neural crest survival and coordinates epithelial–mesenchymal interactions essential for jaw and midline formation.[40–42] Finally, CaM, a calcium-binding transducer interacts with multiple of these pathways (Figure 1) and has an integrative role in osteoblast growth and differentiation[43] and beak shape evolution.[44]

Together these factors and their pathways form an interconnected regulatory network that orchestrates craniofacial patterning during development (Figure 1). For example, in this network, Fgf8 is a central mediator of epithelial patterning and mesenchymal proliferation within the frontonasal region.[38,39] It activates the MAPK–ERK (mitogen-activated protein kinases-extracellular signal-regulated kinases) pathway, and sustained ERK activity suppresses both the Bmp4 Smad cascade as well as Ihh–Gli signaling.[45–47] Bmp4 and Tgfβ2 activate distinct Smad pathways that converge on shared gene regulatory networks, producing synergistic or antagonistic effects on target genes depending on whether they compete for Smad4 or their Smad complexes co-occupy enhancer or promoter regions[48,49] (Figure 1). Wnt4 signaling interacts with all of these pathways by impacting β-catenin dynamics, often inhibiting the canonical Wnt pathway and redirecting β-catenin to the cell membrane, effectively preventing it from reaching the nucleus (Figure 1). However, in some tissue contexts,[31] it can also regulate the canonical Wnt pathway and free β-catenin from its

FIGURE 5 Wnt4, β-catenin, CaM, and Ihh expression at stage HH32. (A) Wnt4 shows relatively weak cytoplasmic expression overall with (1, 2) moderate expression in a large condensation of the maxillary prominence and strong expression in blood cells. (3) Weak expression in mandibular prominence with no expression along its ventral edge, including in the surface epithelium. (4) Surface epithelium shows weak expression. (B) β-catenin shows strong cytoplasmic and nuclear expression in the maxilla and mandible with (1) the strongest nuclear expression just under the surface epithelium of the beak tip. (2) Expression is largely absent in the basihyal cartilage of the mandibular prominence but is present in some nuclei of perichondrogenic cells. (3) Strong nuclear and cytoplasmic expression in the surface epithelium of the mandibular prominence, with particularly strong nuclear expression in adjacent mesenchymal cells and elevated cytoplasmic expression surrounding developing vasculature. (C) CaM shows weak nuclear and cytoplasmic expression in the upper and lower jaw with (1) absence of expression at the beak tip. (2) Weak, mostly cytoplasmic, expression in the emerging Meckel's cartilage with some scattered perinuclear expression. (3) Moderate expression in a region of mesenchyme just below the tongue which is likely pre-myogenic. (D) Ihh shows overall weak cytoplasmic expression in the upper and lower jaw. (1) Expression is largely absent in the epithelium at the tip of the maxillary prominence. (2) Moderate to strong expression in the central condensation of the maxillary prominence. (3) Strong expression in the Meckel's cartilage. See Figure 2 for key to anatomical features and expression patterns. Stain colors as in Figure 3. Scale bars: 50 μm.

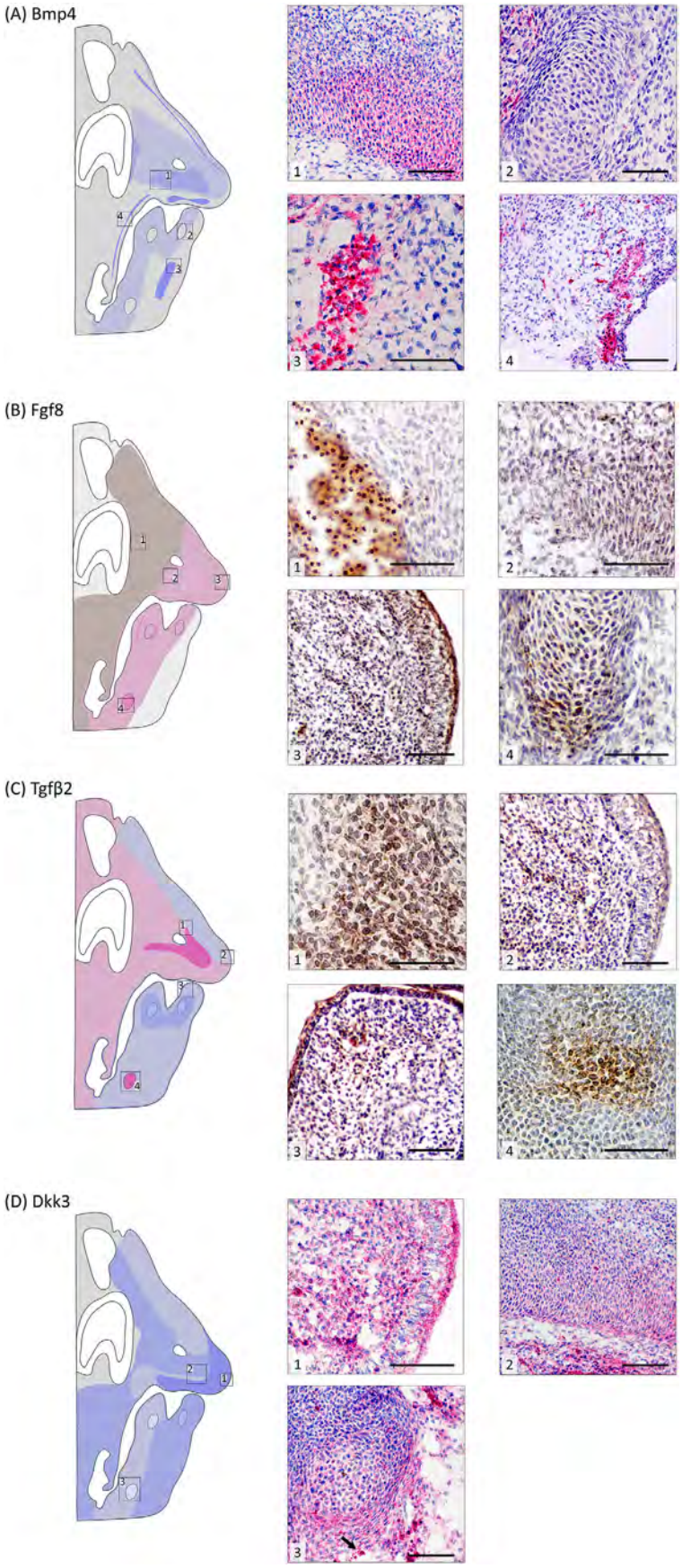

FIGURE 6 Legend on next page.

destruction complex, promoting its movement to the nucleus, where β-catenin co-binds with various transcription factors, including Bmp- and Tgfβ-activated Smads, to regulate numerous craniofacial genes.[7,24,28,31] In turn, Dkk3 can shift Wnt responses toward non-canonical, Ca^{2+}-dependent pathways, engaging CaM signaling[50,51] and it can also prevent β-catenin from entering the nucleus.[52] Importantly, the balance among these pathways is highly context-dependent: the same signaling input can produce opposite transcriptional outcomes depending on Smad availability, Gli activator–repressor ratios, or competition between canonical and non-canonical Wnt branches.[53–55] Yet, how this balance shifts within the context of avian beak morphogenesis, particularly at later stages, is not well characterized.

In this study, we provide an atlas of zebra finch (*Taeniopygia guttata*) beak ontogeny across five developmental stages (Hamburger-Hamilton, HH, 29/30, 32, 36, 39, and 42) that span key late-development transitions in tissue differentiation and bone and cartilage formation. The zebra finch is an emerging model system in developmental biology and neurobiology,[56–59] with high quality genomic resources[60] and well-described developmental staging.[61] Moreover, zebra finches are particularly well suited as a model for developmental studies of the avian beak because their conical beaks share key functional requirements with other well-studied finch and seed-eating birds.[62,63] Using immunohistochemistry with chromogenic labeling and nuclear counterstaining, we map both the spatiotemporal expression and subcellular localization of focal proteins across tissues.

2 | RESULTS AND DISCUSSION

As development proceeds, diffuse mesenchymal expression of proteins transitions to localized, pathway-specific expression, corresponding to morphogenetic patterning and structural maturation of the beak (Figures 2–12). In the earliest stages (HH29-32), most proteins had broad and overlapping expression across epithelial and mesenchymal tissues (Figures 3–6), with the lower jaw showing more variable expression patterns than the upper jaw with heightened expression centered in and around the Meckel's condensation. For example, CaM was expressed in the nuclei in the Meckel's condensation (Figures 3C-2 and 4B-2), Ihh had strong cytoplasmic expression in this region, and Fgf8 had strong perinuclear expression (Table 1). These patterns are consistent with the coordinated role of Fgf8 and Hh signaling in driving cartilage outgrowth during beak development[39] as well as CaM's role in chondrocyte differentiation and maturation.[43] While other studies have found Ca^{2+}/CaM-dependent regulation of nuclear targets in cartilage,[15,64,65] direct visualization of nuclear CaM in early craniofacial condensations has, to our knowledge, not been documented. However, its expression in conjunction with strong Ihh, weak β-catenin, Fgf8 and Tgfβ2 expression within pre-cartilage condensations (Figures 3 and 4) is indicative of a cell population transitioning from pre-condensation mesenchyme to early chondrogenesis (e.g., Sánchez Moreno and Badyaev[66]).

Stage HH32 was a key transition point where regional protein expression begins to define the morphogenetic compartments of upper beak structure (Figures 3–12). With the exception of CaM and β-catenin, all studied

FIGURE 6 Bmp4, Fgf8, Tgfβ2, and Dkk3 expression at stage HH32. (A) Bmp4 shows scattered cytoplasmic expression in upper and lower jaw with (1) moderately strong expression in the large condensation of the maxillary prominence. (2) Emerging cartilage is free of expression. (3) Strong expression in a broad stripe of pre-myogenic cells in the mandibular prominence. (4) The oral epithelium shows weak expression throughout with stripes of strong expression along the oral cavity along the length of the palatine process associated with developing vasculature. (B) Fgf8 expression becomes more widespread at this stage with overall weak cytoplasmic and perinuclear expression throughout. (1) Strong nuclear expression in blood cells with weak cytoplasmic expression in adjacent mesenchyme. (2) Region below nasal cavity of maxillary prominence shows weak cytoplasmic expression with pockets of perinuclear expression. (3) Tip of maxillary prominence shows weak to moderate expression in surface epithelium and the underlying mesenchyme with pockets of perinuclear expression throughout. (4) Strong and largely perinuclear expression in basihyal cartilage. (C) TGF-β2 shows generally weak cytoplasmic expression in the upper and lower beak prominences with areas of strong perinuclear expression. (1) Condensed cells surrounding the nasal cavity area show strong perinuclear expression with posterior cells showing weak cytoplasmic and perinuclear expression while anterior cells show only weak cytoplasmic expression. (2) Weak cytoplasmic expression continues to tip of maxillary prominence. (3) Weak expression in the mesenchyme at the tip of the mandibular prominence with moderate epithelial expression. (4) Strong cytoplasmic and perinuclear expression in the basihyal cartilage formation. (D) Dkk3 shows cytoplasmic expression overall that varies from weak to strong depending on location. (1) Strong expression at the tip of maxillary prominence. (2) Bands of strong, weak and moderate expression (from bottom to top) associated with developing vascular regions, loosely organized mesenchymal cells, and the central condensation of the maxillary prominence, respectively. (3) Strong expression at the edge of the basihyal cartilage with weak expression within. Very strong expression in blood cells (arrow). See Figure 2 for key to anatomical features and expression patterns. Stain colors as in Figure 4. Scale bars: 50 μm.

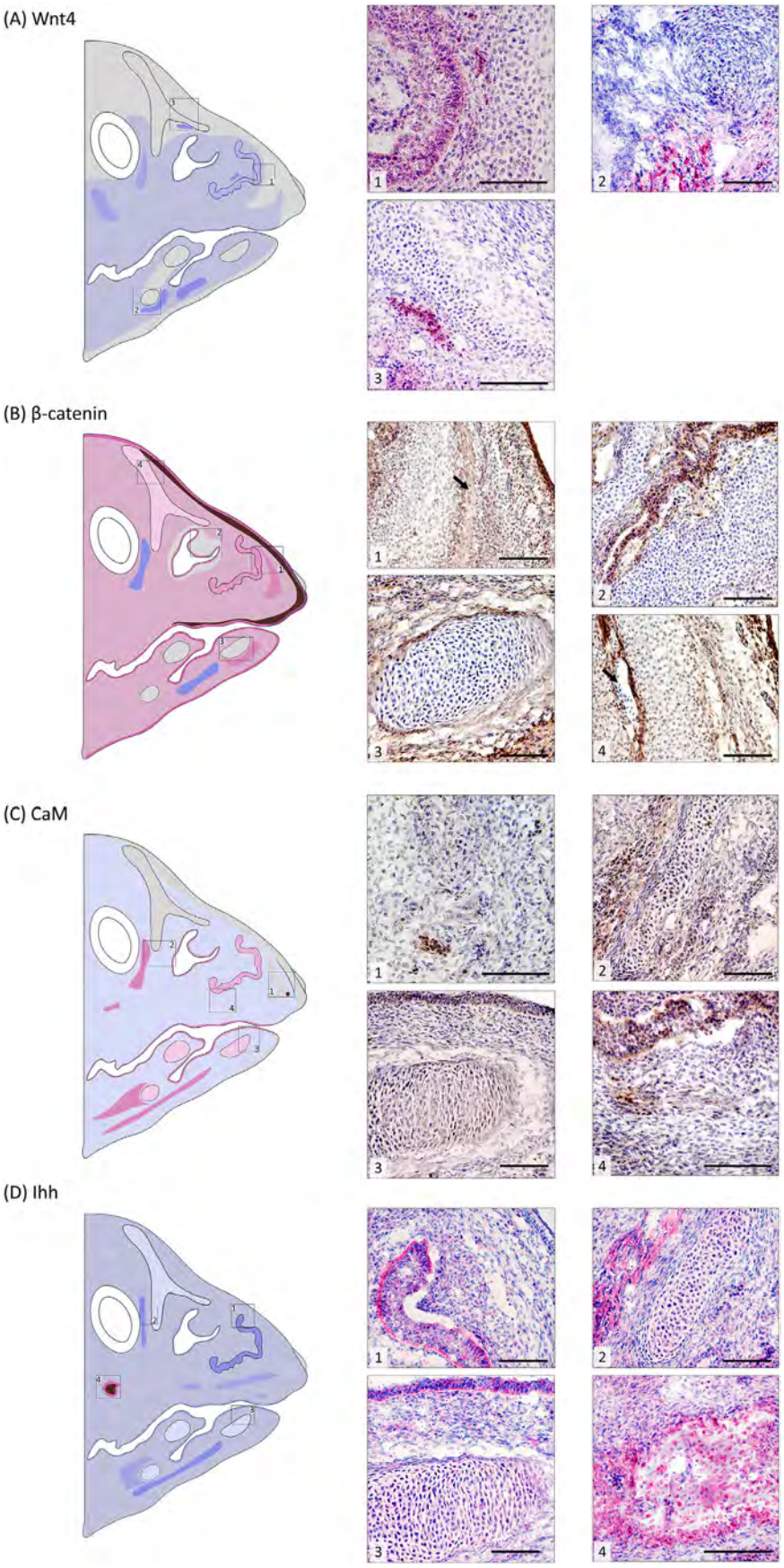

FIGURE 7 Legend on next page.

proteins at this stage had elevated expression around the central condensation of the upper beak (Figures 5 and 6), suggesting that the nasal cavity may be a focal signaling node in upper-beak compartmentalization, similar to the role of the nasal pit in early development.[24,67] Moreover, Dkk3, Fgf8, and β-catenin showed elevated expression toward the beak tip suggesting establishment of proximal-distal patterning and adoption of position-specific regional identities by tissues. These developmental events immediately follow the fusion of the craniofacial prominences which occurs at stage HH28-29 in the chick.[68,69]

By stage HH36, protein expression in the upper jaw became increasingly compartmentalized, with pronounced differentiation among tissue types (Figures 7 and 8). In particular, strong expression of several proteins in myogenic, chondrogenic, and nasal epithelial regions indicates that functionally distinct and tissue-specific signaling environments are forming at this stage. In later stages (HH39–42; Figures 9–12), expression of most proteins was restricted to osteogenic, perichondrogenic, and myogenic domains. Two exceptions were β-catenin and Tgfβ2 which had strong and widespread expression across all stages, although with changing subcellular contexts (Table 1). β-catenin had strong nuclear expression in early stages before shifting to membranous localization in the epithelium at later stages (e.g., Figure 9B-1), while Tgfβ2 tended to have weak cytoplasmic expression in the mesenchyme but shifted to perinuclear expression in both pre-cartilage condensations and regions of active chondrocyte proliferation (e.g., Figure 6C-1,4–). Expression of Fgf8 was spatially restricted at HH29/30 (Figure 4) but underwent a major expansion at stage HH32 (Figure 6), particularly in the upper beak, followed by gradual restriction to epithelial and skeletal boundaries by HH42 (Figure 12). Expression of Ihh, Fgf8, and Tgfβ2 localized to osteogenic fronts, cartilage, and muscle at mid to late stages, with Ihh, particularly, delineating areas of intramembranous ossification (Figures 11 and 12). In contrast, CaM showed weaker and more scattered expression by HH42, with strongest expression in muscle and epithelial cells (Figure 11). Dkk3 was highly expressed at HH29/30 in areas surrounding condensations that would later form cartilage (Figure 4) while Wnt4 expression was the strongest within condensations and absent outside of condensations (e.g., Figures 3 and 5). Thus, early broad expression of regulatory proteins became increasingly compartmentalized, aligning with tissue-specific differentiation and maturation of skeletal, muscular, and epithelial domains in the beak.

2.1 | Shared and divergent expression patterns

The observed patterns of protein expression largely corroborate established interactions among craniofacial gene pathways (Figure 1). For example, β-catenin had strong nuclear expression at the beak tip throughout HH29–36 consistent with its role in maintaining a proliferative growth zone during premaxillary outgrowth.[63] As growth slowed in later stages, β-catenin shifted to strong membranal expression in the surface epithelium consistent with its function in adherens junctions and regulation of epithelial structures.[70] This shift alters the dynamics of underlying mesenchymal cells, for example, by promoting denser packing and reduced motility, thereby

FIGURE 7 Wnt4, β-catenin, CaM, and Ihh expression at stage HH36. (A) Wnt4 shows weak cytoplasmic expression overall with tissue-specific areas of moderate to strong. (1) Moderate expression in the nasal epithelium with weak expression in surrounding cartilage. (2) Strong expression in the myogenic region directly below paraglossal cartilage. (3) Nasal cartilage free of expression, but a pocket of blood cells shows strong expression. (B) β-catenin shows overall weak cytoplasmic and nuclear expression in mesenchyme of both the maxilla and mandible with (1) strong membranal expression in the epithelium of the maxilla tip. Underlying mesenchyme shows alternating bands of strong and weak nuclear/cytoplasmic expression. In the center of this region osteoprogenitor cells (arrow) show moderate cytoplasmic and nuclear expression. (2) Expression is absent in the nasal cartilage but moderate in the nasal epithelium. (3) Meckel's cartilage is free of expression but has a strong band of perichondrogenic expression surrounded by weak to moderate expression in the mesenchyme. (4) Upper region of nasal cartilage exhibits some weak cytoplasmic and nuclear expression. Continued absence of expression in blood cells. (C) CaM shows weak cytoplasmic expression in mesenchyme of both the upper and lower jaw with (1) continued absence of expression at the beak tip and strong nuclear expression in blood cells. (2) Weak, mostly cytoplasmic, expression in the anterior portion of the upper jaw with moderate cytoplasmic and nuclear expression in emerging muscle. (3) Weak perinuclear and cytoplasmic expression in the Meckel's cartilage and its surrounding mesenchyme. Moderate cytoplasmic and perinuclear expression in the overlying oral epithelium. (4) Moderate nuclear and cytoplasmic expression in the nasal epithelium. Emerging osteogenic region (center) shows weak to moderate expression in a few cells. (D) Ihh shows overall weak cytoplasmic expression in the mesenchyme of the upper and lower jaw. (1) Strong cytoplasmic expression in the nasal epithelium. (2) Weak cytoplasmic expression in the nasal cartilage with strong expression in adjacent muscle. (3) Weak expression in the Meckel's cartilage with moderate expression in the overlying oral epithelium. (4) There is strong cytoplasmic and perinuclear expression in the emerging osteogenic region toward the back of the upper jaw. See Figure 2 for key to anatomical features and expression patterns. Stain colors as in Figure 3. Scale bars: 50 μm.

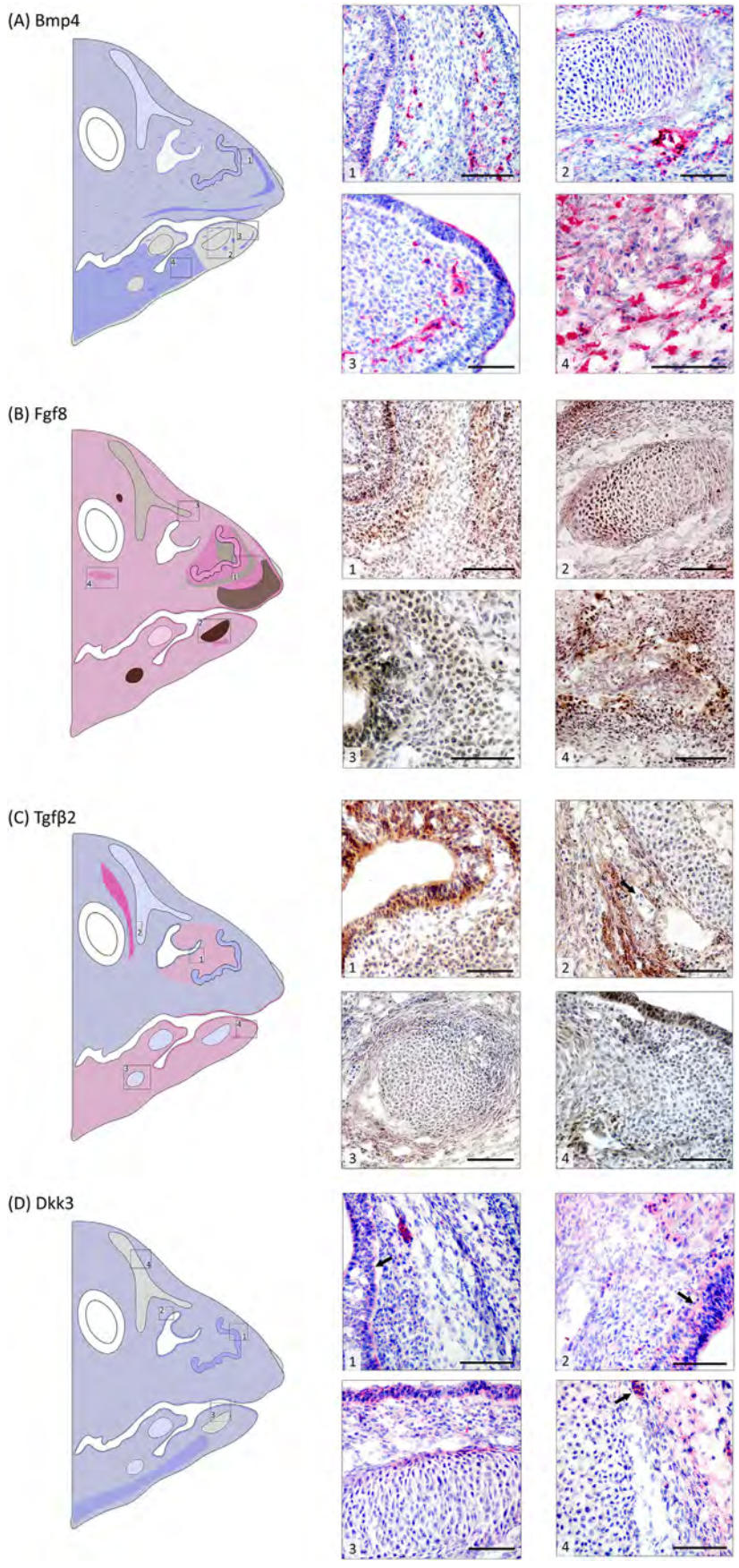

FIGURE 8 Legend on next page.

creating conditions that could favor mechanical activation of Tgfβ2 in the extracellular matrix[71,72] (Figure 1). This process could also modulate the availability of the other extracellular-matrix associated ligands studied here, including Bmp4, Fgf8, Ihh, and Wnt4.[73,74] Dkk3 also shows strong expression at the beak tip at stage HH32, which corroborates its role in regulating premaxillary bone growth downstream of β-catenin and Tgfβ2 signaling.[63,75] Prior work inferring these interactions also showed upregulation of β-catenin and Tgfβ2 signaling at the beak tip[63,75] which differs from our findings as we did not find strong expression of the Tgfβ2 ligand at the beak tip. However, this prior work focused on *TGFβIIr* mRNA expression, not the ligand itself. Instead, we found strong perinuclear expression of Tgfβ2 in the condensation of the upper beak suggesting that ligand production is upregulated more centrally, possibly leading to increased extracellular matrix storage, allowing these cells to function as a source of *latent* TGFβ2 that can act paracrinely on receptor-rich cells at the beak tip.

Additional pathway interactions suggested by prior work (Figure 1) were evident in the early formation of chondrogenic areas. For example, expression of Ihh within pre-chondrogenic condensations and Bmp4 and Tgfβ2 in surrounding regions was consistent with feedback loops in which Ihh/Gli and Bmp/Tgfβ–Smad pathways (Figure 1) jointly regulate chondrocyte proliferation and hypertrophy in cartilage growth plates.[76,77] Likewise, strong nuclear expression of β-catenin in perichondrogenic mesenchyme (e.g., Figure 2B-1) is consistent with its role in preventing premature or excessive chondrocyte differentiation and setting up boundaries between cartilage core areas and surrounding tissues.[78]

The overlap of high Dkk3 and β-catenin in the perichondrogenic region has not been reported before and may indicate a role for Dkk3 in boundary formation, perhaps as a mechanism of buffering against excessive Wnt signaling. Dkk3 is often an antagonist of Wnt/β-catenin signaling[52] however, its role is context-dependent and in this context, it may work with β-catenin to fine-tune Wnt activity. Further work is needed to elucidate Dkk3's role as a potential modulator of Wnt–Bmp/Tgfβ balance at cartilage and bone boundaries. Together, these patterns support many of the canonical points of intersection highlighted by previous studies while revealing potentially novel contributions of CaM and Dkk3 in coordinating formation of early condensations.

We observed strong expression of Ihh, Fgf8, and Tgfβ2 in chondro- and osteogenic tissues, reflecting their coordination of cartilage differentiation and bone matrix formation.[9,32,39,79] In particular, Ihh expression was strong in both central and periosteogenic regions of ossifying tissue, consistent with its dual function in promoting chondrocyte hypertrophy[80,81] and mediating signaling between cartilage and adjacent osteogenic fronts.[82] Perichondrogenic and periosteogenic regions were also enriched in Tgfβ2 and Fgf8, consistent with their roles in the regulation of differentiation at developing cartilage and bone fronts. Bmp4 was notably absent from periosteogenic margins with strong expression in osteogenic centers at stage HH39 (Figure 10A-4). Bmp4 promotes osteogenic differentiation and matrix deposition and its exclusion from this boundary area suggests that its expression may be inhibited at the edges of osteogenic regions to delineate ossification boundaries. Moreover, the strong expression of Bmp4 in the center of this osteogenic tissue likely reflects a vascular channel within the forming

FIGURE 8 Bmp4, Fgf8, Tgfβ2, and Dkk3 expression at stage HH36. (A) Bmp4 shows scattered cytoplasmic expression in upper and lower jaw. (1) Weak expression in the nasal epithelium and typical scattered expression in the adjacent mesenchyme with strong spots of expression interspersed with cells completely free of expression. (2) Meckel's cartilage is free of expression with strong expression in perivascular and blood cells. (3) Tip of mandibular prominence largely free of expression with scattered regions of strong expression. (4) Posterior region of the lower jaw shows moderate to strong expression throughout. (B) Fgf8 expression shows overall weak cytoplasmic and nuclear expression throughout with areas of stronger expression in emerging tissue. (1) Strong nuclear and cytoplasmic expression in the nasal epithelium with bands of nuclear and cytoplasmic expression in adjacent mesenchyme. (2) Meckel's cartilage shows strong nuclear expression, particularly at the periphery. (3) Moderate nuclear to perinuclear expression in the nasal cartilage. (4) Strong nuclear and cytoplasmic expression at an emerging osteogenic region in posterior maxillary prominence. (C) TGF-β2 mesenchymal expression in upper and lower jaw differs in subcellular localization with largely cytoplasmic expression in upper beak while lower beak showed predominantly cytoplasmic and perinuclear expression. (1) Nasal epithelium shows moderate, largely cytoplasmic expression while adjacent cartilage shows more perinuclear expression. (2) Weak cytoplasmic expression in upper nasal cartilage with a band of strong perinuclear and cytoplasmic expression in muscle. Blood cells show no expression (arrow). (3) Weak cytoplasmic and perinuclear expression in the basihyal cartilage with moderately strong perichondrogenic expression. (4) Weak expression in epithelium of the mandibular prominence with regions of mesenchyme showing moderate cytoplasmic and perinuclear expression. (D) Dkk3 shows weak cytoplasmic expression throughout the upper and lower beak mesenchyme. (1, 2) Moderate expression in the nasal epithelium (arrows) compared to surrounding mesenchyme. (3) Meckel's cartilage shows no expression with weak expression in adjacent mesenchyme. Oral epithelium shows moderate expression. (4) Weak expression in surrounding mesenchyme and strong expression in blood cells (arrow). See Figure 2 for key to anatomical features and expression patterns. Stain colors as in Figure 4. Scale bars: 50 μm.

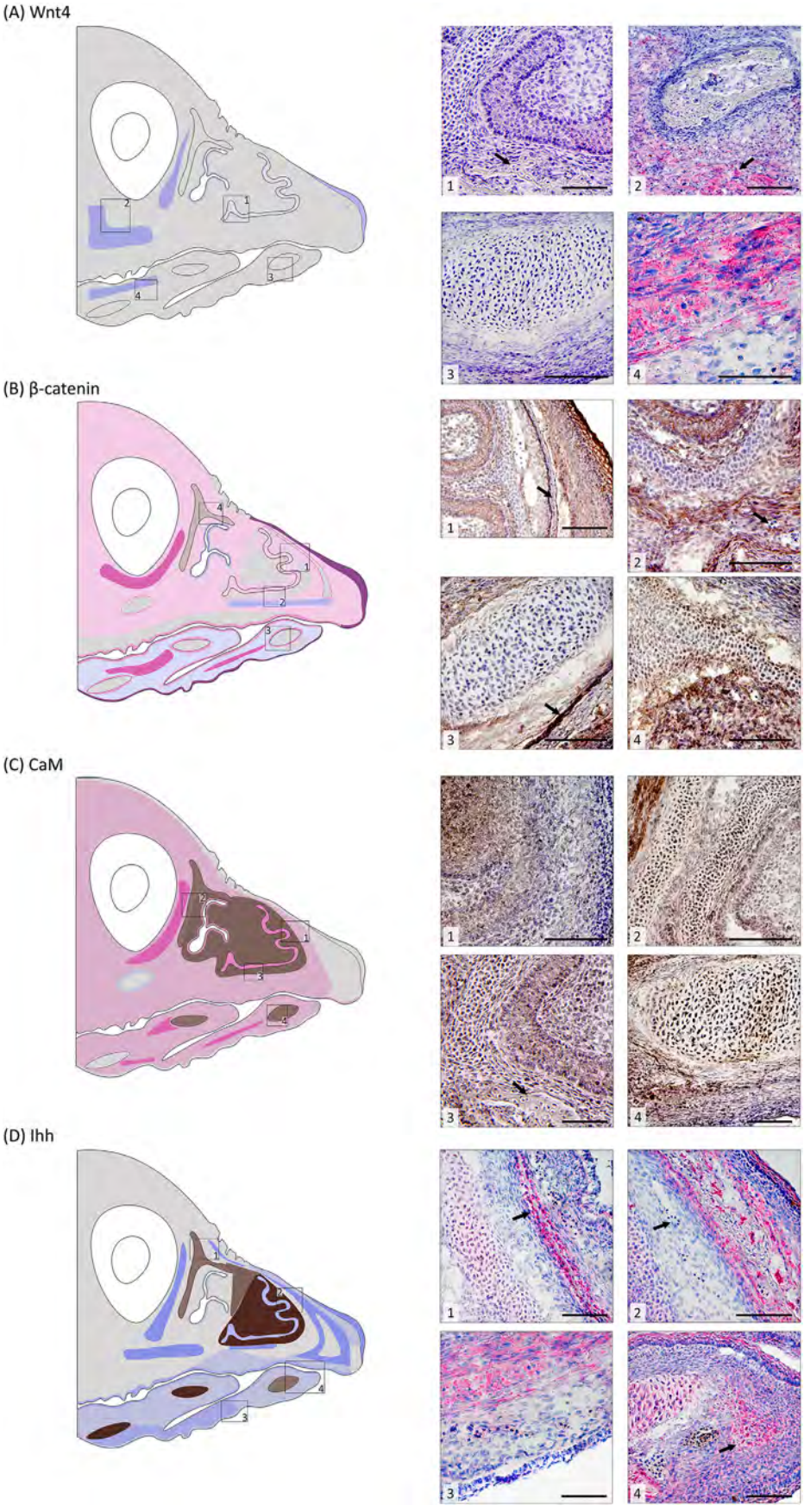

FIGURE 9 Legend on next page.

intramembranous bone. In contrast, β-catenin was strongly expressed in periosteogenic regions and at the margins of the premaxillary cartilage at stage HH42. This latter pattern may reflect its role in promoting differentiation of mesenchymal progenitor cells into osteoblasts while blocking their progression toward chondrocytes.[83,84] Wnt4 was peripherally distributed around osteogenic centers, suggesting a modulatory or signaling feedback role in refining the boundaries of bone-forming regions. Together, these patterns suggest that osteogenesis in the zebra finch beak arises from a coordinated interface between signaling-active boundary cells and differentiating cores, emphasizing that cross-pathway feedback is essential in establishing bone and cartilage differentiation while maintaining boundaries between distinct tissue compartments.

At the subcellular level IHH and TGFβ2 showed consistent perinuclear and FGF8 nuclear expression within chondro- and osteogenic regions, indicating active signaling within differentiating cells, while Bmp4 remained cytoplasmic and was instead associated with osteogenic patterning. Fgf8 is classically characterized as a secreted ligand that signals through cell-surface FGFR pathways.[85] However, studies have proposed intranuclear functions of Fgf proteins, including Fgf8[86] and have found that several Fgf family members have nuclear localization signals[87] which may allow them to migrate into the nucleus and interact with other transcription factors to modulate the expression of target genes.[88] In craniofacial models with perturbed nucleolar function, Fgf8 can influence nuclear processes such as rRNA transcription, such that FGF8-associated effects may extend beyond canonical membrane-initiated signaling.[89] These studies, together with our findings, propose an expanded view of Fgf8's role in craniofacial morphogenesis as a potential transcription coregulator.

2.2 | Spatial and temporal contexts of expression

Developmental dynamics of the lower beak are understudied[90] with available work pointing to pronounced heterochrony related to distinct developmental origins of upper and lower beak tissues, as well as compensatory interactions between them.[26] Similar to prior work, we found that progression of tissue differentiation and patterning of the upper and lower beak differed strongly across developmental stages.[91,92] By HH29/30, condensations had formed in the lower beak with strong expression of several proteins in pre-myogenic and pre-cartilage locations (Table 1), whereas the upper beak exhibited a delayed and more centralized pattern of activity emerging at HH32. After HH32, patterns of expression across the upper and lower beak became more similar with converging subcellular localization of protein expression in chondro- and osteogenic tissues.

FIGURE 9 Wnt4, β-catenin, CaM, and Ihh expression at stage HH39. (A) Wnt4 shows limited cytoplasmic expression in upper and lower beak mesenchyme. (1) Weak expression in the nasal epithelium with no expression in the underlying osteogenic region (arrow). (2) Both the osteogenic center and periosteogenic region are free of expression. Strong expression in the developing muscle below this area (arrow). (3) No expression in Meckel's cartilage and surrounding mesenchyme. (4) Emerging muscle in the lower jaw shows strong expression. (B) β-catenin shows overall weak cytoplasmic and nuclear expression in the mesenchyme of the upper beak and mostly cytoplasmic expression in the lower beak. (1) Bands of weak to moderate cytoplasmic and nuclear expression are associated with the emergence of distinct tissue types in the upper jaw. Cartilage shows mostly nuclear expression, while the nasal epithelium shows mostly cytoplasmic and the mesenchyme shows both. Central areas of the emerging osteogenic region are largely free of expression (arrow) while the edges show a strong band of expression. Surface epithelium shows strong membranal expression. (2) Similar tissue-specific patterns as in 1 with additional views of moderate expression in emerging muscle and no expression in blood cells (arrow). (3) Meckel's cartilage remains free of expression with weak to moderate expression in surrounding mesenchyme. A thin band of cells surrounding the osteogenic envelope shows strong nuclear and cytoplasmic expression (arrow). (4) Upper region of nasal cartilage shows moderate cytoplasmic and nuclear expression. (C) CaM shows weak cytoplasmic and nuclear expression in the mesenchyme of upper and lower jaw with the exception of the upper beak tip. (1) Nuclear and cytoplasmic expression in the nasal epithelium with largely nuclear expression in surrounding cartilage. (2) Strong nuclear expression in nasal cartilage and strong cytoplasmic and nuclear expression in muscle. (3) Similar patterns of tissue expression as in 1 with moderate nuclear and cytoplasmic expression in the osteogenic region (arrow). (4) Strong nuclear expression in Meckel's cartilage with moderate cytoplasmic and nuclear expression in surrounding mesenchyme. Surface epithelium is free of expression. (D) Ihh shows overall limited expression in upper beak mesenchyme with more extensive expression in the lower beak mesenchyme. (1) Weak cytoplasmic expression in the nasal cartilage surrounded by mesenchyme with no expression. An emerging osteogenic region shows strong cytoplasmic expression (arrow). (2) Nasal cartilage with weak perinuclear expression. Adjacent mesenchymal and blood cells are free of expression (arrow) while the osteogenic region shows strong cytoplasmic expression in both the center and periphery. (3) Moderate cytoplasmic expression in muscle of the lower beak. (4) Moderate perinuclear expression in Meckel's cartilage, with moderate expression in the overlying oral epithelium. Mesenchymal expression is mostly weak with pockets of stronger expression in osteogenic regions (arrow). See Figure 2 for key to anatomical features and expression patterns. Stain colors as in Figure 3. Scale bars: 50 μm.

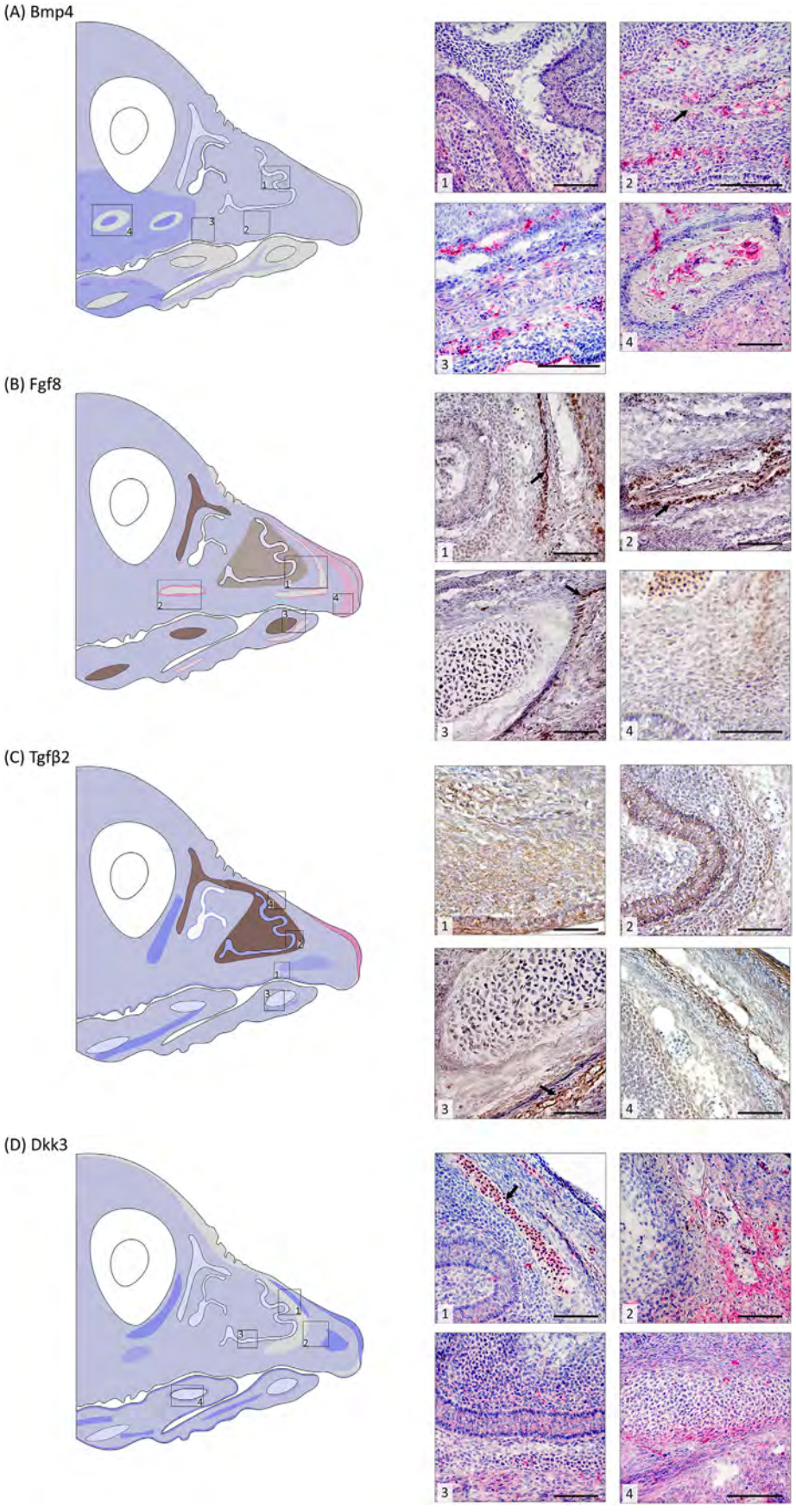

FIGURE 10 Legend on next page.

A notable pattern at stage HH36 was divergence in expression of the oral, surface and nasal epithelia (e.g., see Figure 5C,D). The oral epithelium often showed strong and coordinated patterns of expression in the upper and lower beak that were distinct from the surface epithelium suggesting it may be a coordinating center for growth as well as a source of positional information for tissue differentiation. In the house finch (*Haemorhous mexicanus*), prior to tissue transformations, early arriving neural crest-derived mesenchymal (NCM) cells transiently matched protein profiles of the overlying epithelium producing distinct boundaries that anchor mesenchymal cell condensations.[66] Our findings similarly suggest that epithelial tissue may be an important source of morphogenetic signals that establish patterning in the avian beak.

2.3 | Novel expression patterns in vasculature and blood cells

Bmp4 was strongly expressed in developing vascular regions at multiple stages consistent with its role in endothelial differentiation.[93] Given the emerging view that craniofacial endothelial cells can provide instructive cues during morphogenesis,[94] this pattern raises the possibility that Bmp4 may play a crucial role in patterning during early beak outgrowth. At HH29/30, Bmp4 showed strong expression in linear tracts of vascular tissue that paralleled the ventral edge of the mandible. Because a hypoxic environment is required for chondrogenic differentiation, angiogenesis in the surrounding mesenchyme can limit condensation size.[95] Thus, Bmp4 may influence cartilage size by promoting vascular growth, a process that prepares the way for osteogenesis.[96]

Other proteins (e.g., Wnt4, CaM, Ihh, Fgf8, and Dkk3) were also present in blood cells at the earliest stages. Protein expression patterns are better characterized in definitive erythrocytes than in primitive erythrocytes, and, with the exception of CaM, these proteins are not typically observed in definitive erythrocytes. However, recent studies have found that erythroblasts undergo a drastic shift in protein profile during terminal maturation.[97] While alkaline phosphatase-based chromogens can sometimes give false positives due to endogenous alkaline phosphatase activity, here we used levamisole to minimize this possibility, and our no primary controls run on the same slides were clear (Figure S2). Moreover, we did not observe expression in blood cells for most factors at later stages, which is consistent with a transition to definitive erythroid populations by HH42 in the chick.[98] Finally, these proteins and their pathways are known to regulate the hematopoietic stem cell niche as well as erythropoiesis.[85,99,100] Consistent with this, at HH39, Bmp4 was strongly expressed in vascular spaces inside osteogenic tissue which likely reflects the establishment of the hematopoietic niche as this is consistent with timing of onset of hematopoiesis in primary bone marrow of chick embryos.[101]

2.4 | Conclusions

In this study, we bridge molecular and histological perspectives, providing a foundation for understanding how

FIGURE 10 Bmp4, Fgf8, Tgfβ2, and Dkk3 expression at stage HH39. (A) Bmp4 shows weak cytoplasmic expression in the upper jaw with a gradient of no expression, weak expression, and moderate expression from the tip to the back of the lower jaw. (1) Weak expression in the nasal epithelium with some scattered expression in the adjacent cartilage. (2) Weak expression in upper jaw mesenchyme with strong expression in the emerging osteogenic region (arrow). (3) Weak expression in muscle of the lower jaw with areas of strong expression directly adjacent to and at the bottom edge of the tongue. Epithelial tissue is largely free of expression. (4) An osteogenic region of the upper beak shows strong signal within a central vascular space with little to no staining in osteogenic tissue and a surrounding ring of mesenchymal cells. Away from this osteogenic region, mesenchyme shows weak cytoplasmic expression. (B) Fgf8 expression shows weak cytoplasmic expression in most of the upper and lower jaw mesenchyme. (1) Weak cytoplasmic expression in the nasal epithelium with bands of weak perinuclear expression in adjacent cartilage. (2) Strong perinuclear and cytoplasmic expression in the periphery of an osteogenic region (arrow). (3) Moderate perinuclear expression in Meckel's cartilage with very weak cytoplasmic expression in the surrounding mesenchyme with heightened expression in an emerging osteogenic region (arrow). (4) The upper beak tip is the only mesenchymal region to show strong perinuclear and cytoplasmic expression. (C) TGF-β2 mesenchymal expression in upper and lower jaw shows largely cytoplasmic expression overall. (1) Moderate cytoplasmic expression in epithelium and mesenchyme with weak and scattered expression in the osteogenic region. Blood cells are free of expression. (2) Strong cytoplasmic expression in nasal epithelium with strong perinuclear expression in the adjacent cartilage. (3) Meckel's cartilage shows very weak cytoplasmic expression with moderately strong expression in the adjacent osteogenic region (arrow). (4) Strong perinuclear expression in nasal cartilage and in nearby osteogenic region with only weak cytoplasmic expression in mesenchyme and surface epithelium. (D) Dkk3 shows weak cytoplasmic expression throughout the upper and lower beak mesenchyme. (1) Weak expression in the nasal epithelium and moderate expression in blood cells (arrow). (2) Strong expression in the osteogenic region of the emerging premaxillary bone. (3) Weak to moderate expression in nasal epithelium and its surrounding cartilage in more posterior regions of the upper beak. (4) Paraglossal shows some weak expression with stronger expression at the ventral edge. See Figure 2 for key to anatomical features and expression patterns. Stain colors as in Figure 4. Scale bars: 50 μm.

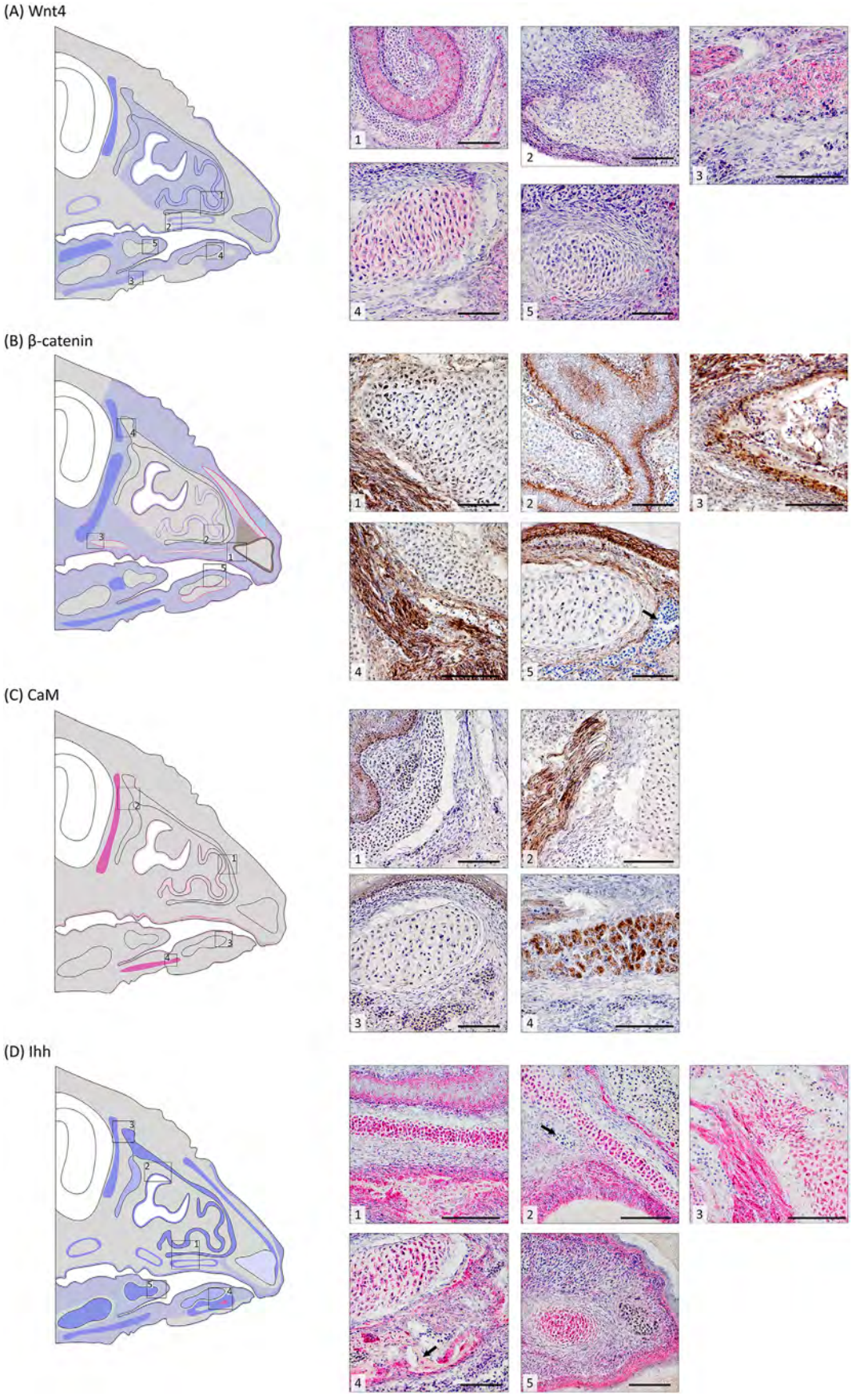

FIGURE 11 Legend on next page.

signaling dynamics are translated into morphological form. By documenting cellular colocalization of protein expression in its tissue-level context we reveal points of pathway convergence for proliferative, chondrogenic, and osteogenic phases of avian beak development. By mapping eight core regulatory proteins across five developmental stages and multiple tissue types, our study extends previous work that examined these factors at the transcript level or only at early stages, offering the first systematic depiction of how signaling activity changes across the maturation of the beak. Bridging molecular and histological perspectives provides a synthesis for the timing and specification of tissue transformations, not just in later stages of beak development but also across the upper and lower beak, two current gaps in the field. Ultimately, our map will provide a foundation for comparative studies of craniofacial development as well as evolution of the avian beak.

3 | EXPERIMENTAL PROCEDURES

3.1 | Embryo collection, staging, and histology

Zebra finches were housed in a large semi-outdoor (roofed with open wire mesh on two sides) walk-in aviary (4.72L × 1.52W × 2.44H m) at the University of Arizona in accordance with the Institutional Animal Care and Use Committee's guidance and approval (IACUC: 16-111). In this colony, which houses from 80 to 100 zebra finches at any given time, individuals are allowed to pair freely and breeding is closely monitored. Throughout breeding, birds receive finch mix seed and water ad libitum, in addition to grit, calcium supplements, prophylactic coccidiosis medication (preventative maintenance dosage, semi-weekly), weekly millet spray, and twice-weekly dietary supplements of spinach and hard-boiled egg. Nest boxes in the colony were checked daily for fresh eggs, which were marked during laying to keep track of laying order and developmental timing. Collected embryos were viewed under a dissecting scope to confirm embryo stage.[61] Five stages spaced throughout the final third of development were chosen for sectioning (HH29/30, HH32, HH36, HH39, and HH42; $n = 10$). Many of the embryos at stage 29/30 were collected midway between these two stages and so are lumped for analysis. After staging, embryos were fixed and stabilized using PaxGene (Pre-Analytix, Switzerland) and dehydrated in 30% sucrose in PBS. The heads of embryos were flash frozen in dimethylbutane and placed in OCT media (Fisher Scientific, Itasca, IL) before cryosectioning at 10–12 μm. Slides were stored at −80°C until immunohistochemistry (IHC). Before IHC, we identified the approximate midline of each embryo to standardize location for tissue staining. Eight sections per stage were stained with hematoxylin and eosin using standard procedures to differentiate among tissue types and visualize tissue transformation across developmental time[74] (H&E; U. Rochester MC).

We assess expression patterns across the following tissue types/regions: We refer to the cartilage-adjacent mesenchymal zone as "perichondrogenic" as an operational spatial domain.

FIGURE 11 Wnt4, β-catenin, CaM, and Ihh expression at stage HH42. (A) Wnt4 is largely absent in upper beak mesenchyme with limited expression in the lower beak mesenchyme. (1) Moderate expression in the nasal epithelium and weak expression in surrounding cartilage. (2) Osteogenic center is free of expression while periosteogenic area shows weak expression. (3) Moderate expression in muscle of lower jaw while surrounding mesenchyme is largely free of expression. (4) Weak cytoplasmic expression in the Meckel's cartilage. (5) Paraglossal cartilage is largely free of expression. (B) β-catenin shows overall weak cytoplasmic expression in mesenchyme of the upper and lower beak. (1) Premaxillary cartilage center is free of expression with strong nuclear expression at edges. (2) Nasal epithelium shows moderate expression at its base, while surrounding cartilage is free of expression. (3) Muscle (top left) and osteogenic regions show strong cytoplasmic and nuclear expression. (4) Upper nasal cartilage is largely free of expression with some weak expression at edges. (5) Meckel's cartilage is free of expression and strong cytoplasmic and membranal expression continues in epithelial tissues. Blood cells show no expression (arrow). (C) CaM shows no expression in mesenchyme of upper and lower jaw. (1) Weak nuclear and cytoplasmic expression in nasal epithelium. (2) Strong nuclear and cytoplasmic expression in muscle. (3) No expression in Meckel's cartilage with weak cytoplasmic and nuclear expression in overlying epithelium. (4) Strong cytoplasmic and nuclear expression in muscle of lower beak. (D) Ihh shows overall limited expression in upper beak mesenchyme with more extensive expression in the lower beak mesenchyme. (1) Strong cytoplasmic expression in the nasal epithelium, nasal cartilage and in an underlying periosteogenic region. (2) Nasal cartilage and epithelium show strong expression while blood cells (arrow) show no expression. (3) Strong expression in muscle and nearby upper nasal cartilage. (4) Strong cytoplasmic expression in the Meckel's cartilage, with moderate expression in surrounding mesenchyme. Osteogenic region (arrow) shows both cytoplasmic and perinuclear expression at its center. (5) Strong expression in paraglossal cartilage with a notable absence of expression in perichondrogenic area. Moderate expression in epithelium of tongue. See Figure 2 for key to anatomical features and expression patterns. Stain colors as in Figure 3. Scale bars: 50 μm.

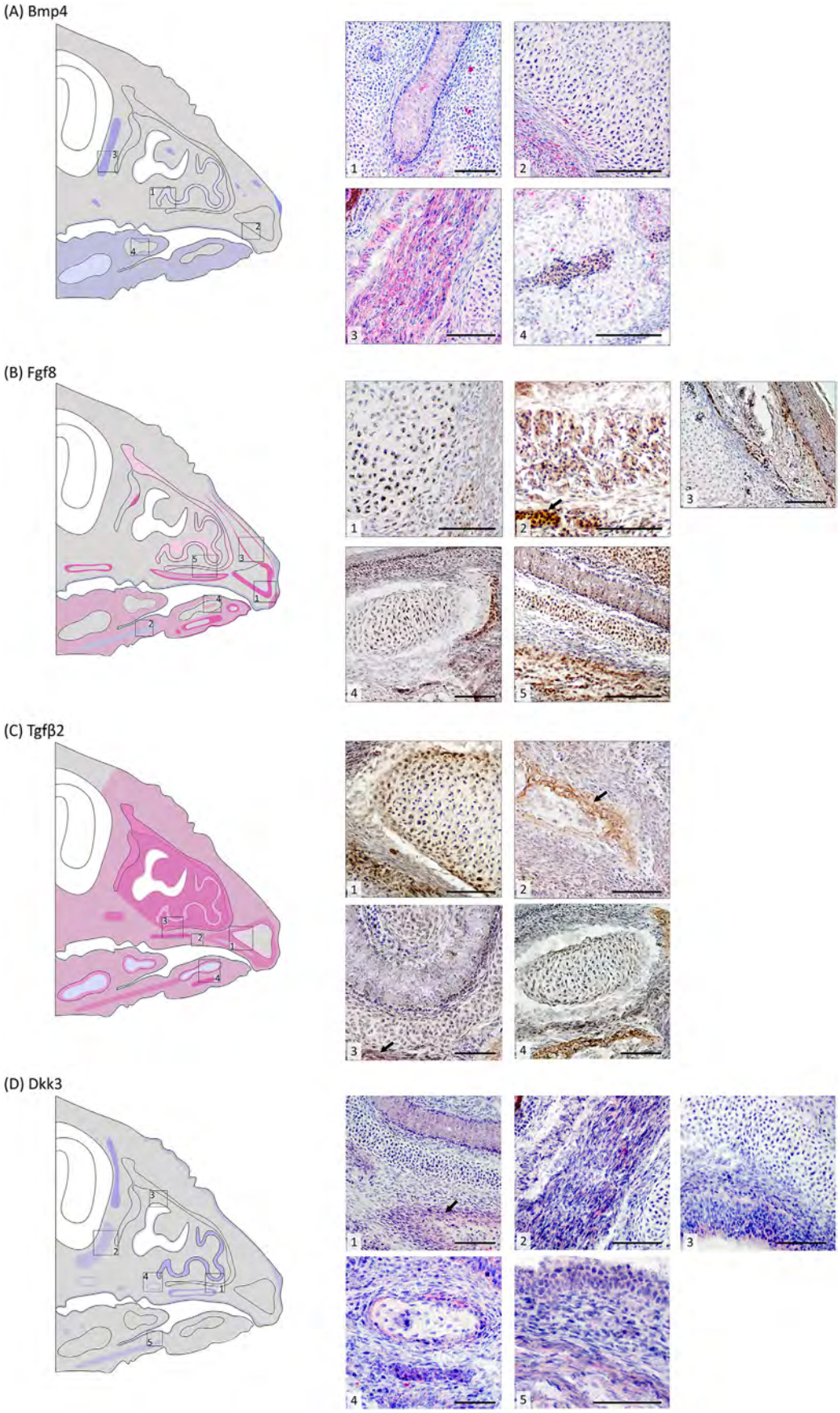

FIGURE 12 Legend on next page.

3.2 | Immunohistochemistry

IHC was optimized for eight antibodies (Table S1) using positive and negative control tissue (esophagus, kidney, esophagus, testes, and small intestine) collected and sectioned as described above (Table S1, Figure S1) as well as isotype controls (Cell Signaling Technologies, Danvers, MA; see References [66,73] for details).

For immunostaining, we used anti-β-catenin (610153, 1:16,000, BD Transduction Laboratories), anti-CaM (sc-137079, 1:15, Santa Cruz Biotechnology), anti-Wnt4 (ab91226, 1:800; Abcam), anti-Tgfβ2 (ab36495, 1:800, Abcam), anti-Bmp4 (ab118867, 1:100, Abcam), anti-Ihh (ab184624, 1:100, Abcam), anti-Dkk3 (ab214360, 1:100, Abcam), and anti-Fgf8 (89550, 1:50, Abcam) antibodies using methods described previously.[102] Validations confirming specificity of stains including isotype, no primary and no secondary controls, are provided in Badyaev et al.[73] In the present study, we additionally included slide-level negative controls for every embryo and antibody grouping: on each slide, a matched control section was processed in parallel with omission of the primary antibody ("no primary"), while all subsequent steps (secondary antibodies, ABC reagents, and chromogen/substrate development) were identical. Reactions were visualized with either diaminobenzidine (DAB, Elite ABC HRP Kit, PK-6100, Vector Labs) or Vector Red Alkaline Phosphatase substrate with 1.3 mM levamisole added in combination with VECTASTAIN ABC-AP Kit (AK-5000, Vector Labs). Slides were counterstained with Mayer's hematoxylin, blued in ammonium water, dehydrated, cleared, and mounted with Permount mounting medium (Fisher Scientific) prior to analysis. Three slides, each containing four tissue sections (12 sections per embryo) were run with the following grouped antibodies: (i) β-catenin, Fgf8, Tgfβ2 and no primary control, (ii) Bmp4, Wnt4, Ihh and no primary control, and (iii) Dkk3 and no primary control, and CaM and no primary control. The control sections on each slide did not receive the primary antibody during IHC but were otherwise treated the same as other sections and showed minimal signal (see Figure S2).

3.3 | Photomicroscopy and image assessment

IHC staining was visualized with brightfield optics (Olympus microscope, Japan). Pictures were taken with a microscope digital camera (Olympus DP74) and the Olympus cellSens software. All images were taken at standardized settings to ensure consistency across slides. Images were taken at low magnification (4× and 10×) to summarize patterns throughout the upper and lower beak and at high magnifications (20× and 40×) to show cellular level details. For each stage, two individuals were sectioned and stained, and within each individual, staining patterns were assessed for consistency across multiple IHC runs (2–4 runs per individual). We then created a consensus staining pattern from these images, documenting presence/absence of expression, cellular localization, and types of tissues stained. Qualitative assessments of high, medium, and low levels of expression were based on comparison of relative expression levels within sections only. A consensus map of expression was determined based on the maximum area

FIGURE 12 Bmp4, Fgf8, Tgfβ2, and Dkk3 expression at stage HH42. (A) Bmp4 shows no mesenchymal expression in the upper beak with weak to moderate expression in the lower beak. (1) Weak expression in the nasal epithelium. (2) Weak expression in the epithelium underlying the premaxillary cartilage. (3) Strong expression in upper jaw muscle. Adjacent cartilage is largely free of expression. (4) Osteogenic region of paraglossal shows no expression; however, a vascular chamber in the center shows some very light expression in blood cells. Limited scattered expression in the mesenchyme and the oral epithelium. (B) Fgf8 expression shows overall no expression in most of the upper jaw mesenchyme with weak perinuclear and cytoplasmic expression in the lower jaw. (1) Strong perinuclear expression at the edges of the premaxillary cartilage and perinuclear/cytoplasmic expression at the beak tip. (2) Moderate cytoplasmic expression in muscle of the lower beak with strong expression in blood cells (arrow). (3) Strong periosteogenic expression in the upper beak and weak expression in the surface epithelium. (4) Meckel's cartilage shows strong nuclear expression in center with no expression in perichondrogenic area. (5) Weak cytoplasmic and nuclear expression in the nasal epithelium, weak nuclear expression in the nasal cartilage and strong nuclear expression in adjacent osteogenic area. (C) Tgfβ2 mesenchymal expression in upper and lower beaks shows weak cytoplasmic and perinuclear expression overall. (1) Strong expression in perichondrogenic region of pre-maxillary with additional weak expression at cartilage edges. (2) Weak to moderate expression in mesenchyme and osteogenic region (arrow) of upper beak. (3) Expression varies from weak in epithelium to moderate in surrounding cartilage to strong in muscle (arrow). (4) Meckel's cartilage is largely free of expression with some weak cytoplasmic expression, especially around edges. (D) Dkk3 shows limited expression throughout the upper and lower beak mesenchyme. (1) Weak expression in the nasal epithelium in the periosteogenic region (arrow). (2) Weak expression in muscle. (3) Weak to no expression at edge of nasal epithelium. (4) Weak to moderate periosteogenic expression in upper beak. (5) Weak expression in oral epithelium and muscle of lower jaw. See Figure 2 for key to anatomical features and expression patterns. Stain colors as in Figure 4. Scale bars: 50 μm.

TABLE 1 Cellular localization of protein expression across developmental stages in upper and lower jaw.

		Upper jaw								Lower jaw							
Stage	**Tissue**	**Wnt4**	***β*-cat**	**CaM**	**Ihh**	**Bmp4**	**Fgf8**	**Tgf*β*2**	**Dkk3**	**Wnt4**	***β*-cat**	**CaM**	**Ihh**	**Bmp4**	**Fgf8**	**Tgf*β*2**	**Dkk3**
29/30	Mesenchymal	C	CN	CN	C	C	C	C	C	C	CN	CN	C	C	C	CP	C
	Epithelial	C	CN	C	C	C		C	C	C	CN	C	C	C	C	C	C
	Blood cells	CP		N	CP	CP	N		CP				CP	C	N		CP
	Chondrogenic[a]	-	-	-	-	-	-	-	-	C	C	CN	C	C	CP	C	C
	Perichondrogenic[a]	-	-	-	-	-	-	-	-	C	CN	CN	C		CP	CP	C
	Myogenic	-	-	-	-	-	-	-	-	-	CN	CN	C	-	-	-	C
32	Mesenchymal	C	CN	CN	C	C	CP	CP	C	C	CN	CN	C	C	C	C	C
	Epithelial	C	CN	CN	C	C	CP	C	C	C	CN	CN	C	C	C	C	C
	Blood cells	C		N	C	C	CN		CN	C		N	C	C	CP		CN
	Chondrogenic	-	-	-	-	-	-	-	-	C		CP	C		CP	CP	
	Perichondrogenic	-	-	-	-	-	-	-	-	C	CN				C	C	C
	Myogenic	-	-	-	-	-	-	-	-	C	CN	CN	C	C	C	-	C
36	Mesenchymal	C	CN	C	C	C	CN	CP	C	C	CN	C	C	C	CN	C	C
	Epithelial	C	CNM	CP	C	C	CN	CP	C	C	CN	CP	C	C	CN	CP	C
	Blood cells	C		N	C	C	N		C	C		N	C	C	N		C
	Chondrogenic	C	CN		C	C	CN	CP	C			CP	C		CN	C	C
	Perichondrogenic		CN				CN	CP			CN				CN	CP	C
	Myogenic	C	C	CN	C	C	-	CP	-		CN	CN	C	C	-	CP	C
	Osteogenic		CN	CN	CP		CN	C	C	-	CN	-	-	-	CN	-	-
	Periosteogenic	C	CN		CP		CN	C	C	-	CN	-	-	-	CN	-	-
39	Mesenchymal	C	CN	CN		C	CP	C	C		C	CN	C	C	C	C	C
	Epithelial	C	CNM	CN	C	C	C	C	C		CNM	CN	C		C	C	C
	Blood cells	C		N	C	C			C			N	C	C			C
	Chondrogenic		N	N	P	C	P	P	C			N	CP		P	C	C
	Perichondrogenic		CN	CN		C	C	C	C		CN	CN				C	C
	Myogenic	C	CN	CN	C	C	-	-	C	C	CN	CN	C	C	-	C	C
	Osteogenic				C	C		C	C			N	CP			C	-
	Periosteogenic	C	CN	CN	C		CP				CN	CN	CP		CP		-
42	Mesenchymal		C					CP		C	C		C	C	CP	CP	
	Epithelial	C	CNM	CN	C	C	CP	CP	C	C	CNM	CN	C	C	C	CP	C

TABLE 1 (Continued)

Stage	Tissue	Upper jaw							Lower jaw						
		Wnt4	β-cat	CaM	Ihh	Bmp4	Fgf8	Tgfβ2	Dkk3	Wnt4	β-cat	CaM	Ihh	Bmp4	Fgf8	Tgfβ2	Dkk3
	Blood cells					C				C				C	CP		
	Chondrogenic	C	N		C		P	CP		C			C	C	P	C	
	Perichondrogenic		N					CP			CN					CP	
	Myogenic	C	C	CN	C	C		CP	C	C	C	CN	C	C	C	CP	C
	Osteogenic				C		NP	CP					CP		P	CP	
	Periosteogenic	C	CN		C			CP	C		CN		C		CN	CP	

Abbreviations: **C**, cytoplasmic; **M**, membranal; **N**, nuclear; **P**, perinuclear; Blank, no expression; -, no sample with tissue.
[a]Denotes pre-cartilage condensation and perichondrogenic progenitor cells at this stage.

stained across different individuals and sections, and the most inclusive subcellular localization designation was used for Table 1.

ACKNOWLEDGMENTS

We thank Fatima Bravo for help with IHC assays and Neha Varshney for assistance with histological identification. The Badyaev and Duckworth lab groups provided helpful feedback that improved this manuscript. This project was supported by grants from the National Science Foundation (IBN-0218313 and DEB-1754465) to A.V.B.

FUNDING INFORMATION

This project was supported by grants from the National Science Foundation (IBN-0218313 and DEB-1754465).

CONFLICT OF INTEREST STATEMENT

The authors declare no conflicts of interest.

DATA AVAILABILITY STATEMENT

The data that supports the findings of this study are available in the supplementary material of this article as well as the article tables and figures.

REFERENCES

1. Kholodenko BN. Cell signalling dynamics in time and space. *Nat Rev Mol Cell Biol*. 2006;7:165-176.
2. Wolpert L. Positional information and patterning revisited. *J Theor Biol*. 2011;269(1):359-365. doi:10.1016/j.jtbi.2010.10.034
3. Mosby LS, Bowen AE, Hadjivasiliou Z. Morphogens in the evolution of size, shape and patterning. *Development*. 2024;151(18):1–14. doi:10.1242/dev.202412
4. Aponte JD, Katz DC, Roth DM, et al. Relating multivariate shapes to genescapes using phenotype-biological process associations for craniofacial shape. *Elife*. 2020;10:e68623. doi:10.7554/eLife.68623
5. Alvarez M, Rhodes SJ, Bidwell JP. Context-dependent transcription: all politics is local. *Gene*. 2003;313:43-57. doi:10.1016/s0378-1119(03)00627-9
6. Lu J, Wu T, Zhang B, et al. Types of nuclear localization signals and mechanisms of protein import into the nucleus. *Cell Commun Signal*. 2021;19(1):60. doi:10.1186/s12964-021-00741-y
7. Basson MA. Signaling in cell differentiation and morphogenesis. *Cold Spring Harb Perspect Biol*. 2012;4(6):1–21. doi:10.1101/cshperspect.a008151
8. Downward J. The ins and outs of signalling. *Nature*. 2001;411:759-762.
9. Schneider RA. Cellular, molecular, and genetic mechanisms of avian beak development and evolution. *Annu Rev Genet*. 2024;58:433-454. doi:10.1146/annurev-genet-111523-101929
10. Munro V, Kelly V, Messner CB, Kustatscher G. Cellular control of protein levels: a systems biology perspective. *Proteomics*. 2024;24(12–13):e2200220. doi:10.1002/pmic.202200220

11. Ghazalpour A, Bennett B, Petyuk VA, et al. Comparative analysis of proteome and transcriptome variation in mouse. *PLoS Genet*. 2011;7(6):e1001393. doi:10.1371/journal.pgen.1001393
12. Velez-Bermudez IC, Schmidt W. The conundrum of discordant protein and mRNA expression. Are plants special? *Front Plant Sci*. 2014;5:619. doi:10.3389/fpls.2014.00619
13. Asplund A, Edqvist PH, Schwenk JM, Ponten F. Antibodies for profiling the human proteome-the human protein atlas as a resource for cancer research. *Proteomics*. 2012;12(13):2067-2077. doi:10.1002/pmic.201100504
14. Abramyan J, Richman JM. Craniofacial development: discoveries made in the chicken embryo. *Int J Dev Biol*. 2018;62(1-2-3):97-107. doi:10.1387/ijdb.170321ja
15. Parsons KJ, Albertson RC. Roles for Bmp4 and CaM1 in shaping the jaw: evo-devo and beyond. *Annu Rev Genet*. 2009;43:369-388. doi:10.1146/annurev-genet-102808-114917
16. Szabo-Rogers HL, Smithers LE, Yakob W, Liu KJ. New directions in craniofacial morphogenesis. *Dev Biol*. 2010;341(1):84-94. doi:10.1016/j.ydbio.2009.11.021
17. Helms JA, Cordero D, Tapadia MD. New insights into craniofacial morphogenesis. *Development*. 2005;132(5):851-861. doi:10.1242/dev.01705
18. Fox SC, Waskiewicz AJ. Transforming growth factor beta signaling and craniofacial development: modeling human diseases in zebrafish. *Front Cell Dev Biol*. 2024;12:1338070. doi:10.3389/fcell.2024.1338070
19. Lin GL, Hankenson KD. Integration of BMP, Wnt, and notch signaling pathways in osteoblast differentiation. *J Cell Biochem*. 2011;112(12):3491-3501. doi:10.1002/jcb.23287
20. Roth DM, Bayona F, Baddam P, Graf D. Craniofacial development: neural crest in molecular embryology. *Head Neck Pathol*. 2021;15(1):1-15. https://doi.org10.1007/s12105-021-01301-z
21. Campas O, Mallarino R, Herrel A, Abzhanov A, Brenner MP. Scaling and shear transformations capture beak shape variation in Darwin's finches. *Proc Natl Acad Sci USA*. 2010;107(8):3356-3360. doi:10.1073/pnas.0911575107
22. Merrill AE, Eames BF, Weston SJ, Heath T, Schneider RA. Mesenchyme-dependent BMP signaling directs the timing of mandibular osteogenesis. *Development*. 2008;135(7):1223-1234. doi:10.1242/dev.015933
23. Wu P, Jiang TX, Shen JY, Widelitz RB, Chuong CM. Morphoregulation of avian beaks: comparative mapping of growth zone activities and morphological evolution. *Dev Dyn*. 2006;235(5):1400-1412. doi:10.1002/dvdy.20825
24. Geetha-Loganathan P, Nimmagadda S, Antoni L, et al. Expression of WNT signalling pathway genes during chicken craniofacial development. *Dev Dyn*. 2009;238(5):1150-1165. doi:10.1002/dvdy.21934
25. Dao DY, Jonason JH, Zhang Y, et al. Cartilage-specific beta-catenin signaling regulates chondrocyte maturation, generation of ossification centers, and perichondrial bone formation during skeletal development. *J Bone Miner Res*. 2012;27(8):1680-1694. doi:10.1002/jbmr.1639
26. Cheng Y, Miller MJ, Lei F. Molecular innovations shaping beak morphology in birds. *Annu Rev Anim Biosci*. 2025;13(1):99-119. doi:10.1146/annurev-animal-030424-074906
27. Lawson LP, Petren K. The adaptive genomic landscape of beak morphology in Darwin's finches. *Mol Ecol*. 2017;26(19):4978-4989. doi:10.1111/mec.14166
28. Xue C, Chu Q, Shi Q, Zeng Y, Lu J, Li L. Wnt signaling pathways in biology and disease: mechanisms and therapeutic advances. *Signal Transduct Target Ther*. 2025;10(1):106. doi:10.1038/s41392-025-02142-w
29. Liu F, Kohlmeier S, Wang CY. Wnt signaling and skeletal development. *Cell Signal*. 2008;20(6):999-1009. doi:10.1016/j.cellsig.2007.11.011
30. Chen L, Wang K, Shao Y, et al. Structural insight into the mechanisms of Wnt signaling antagonism by Dkk. *J Biol Chem*. 2008;283(34):23364-23370. doi:10.1074/jbc.M802375200
31. Zhang Q, Pan Y, Ji J, Xu Y, Zhang Q, Qin L. Roles and action mechanisms of WNT4 in cell differentiation and human diseases: a review. *Cell Death Discov*. 2021;7(1):287. doi:10.1038/s41420-021-00668-w
32. Chen G, Deng C, Li YP. TGF-beta and BMP signaling in osteoblast differentiation and bone formation. *Int J Biol Sci*. 2012;8(2):272-288. doi:10.7150/ijbs.2929
33. Grafe I, Alexander S, Peterson JR, et al. Tgf-beta family signaling in mesenchymal differentiation. *Cold Spring Harb Perspect Biol*. 2018;10(5):1–49. doi:10.1101/cshperspect.a022202
34. Kahata K, Dadras MS, Moustakas A. TGF-beta family signaling in epithelial differentiation and epithelial-mesenchymal transition. *Cold Spring Harb Perspect Biol*. 2018;10(1):1–31. doi:10.1101/cshperspect.a022194
35. Dailey L, Ambrosetti D, Mansukhani A, Basilico C. Mechanisms underlying differential responses to FGF signaling. *Cytokine Growth Factor Rev*. 2005;16(2):233-247. doi:10.1016/j.cytogfr.2005.01.007
36. Su N, Jin M, Chen L. Role of FGF/FGFR signaling in skeletal development and homeostasis: learning from mouse models. *Bone Res*. 2014;2:14003. doi:10.1038/boneres.2014.3
37. Tuzon CT, Rigueur D, Merrill AE. Nuclear fibroblast growth factor receptor signaling in skeletal development and disease. *Curr Osteoporos Rep*. 2019;17(3):138-146. doi:10.1007/s11914-019-00512-2
38. Firnberg N, Neubuser A. FGF signaling regulates expression of Tbx2, erm, Pea3, and Pax3 in the early nasal region. *Dev Biol*. 2002;247(2):237-250. doi:10.1006/dbio.2002.0696
39. Abzhanov A, Tabin CJ. Shh and Fgf8 act synergistically to drive cartilage outgrowth during cranial development. *Dev Biol*. 2004;273(1):134-148. doi:10.1016/j.ydbio.2004.05.028
40. St-Jacques B, Hammerschmidt M, McMahon AP. Indian hedgehog signaling regulates proliferation and differentiation of chondrocytes and is essential for bone formation. *Genes Dev*. 1999;13:2072-2086.
41. Dworkin S, Boglev Y, Owens H, Goldie SJ. The role of sonic hedgehog in craniofacial patterning, morphogenesis and cranial neural crest survival. *J Dev Biol*. 2016;4(3):1–12. doi:10.3390/jdb4030024
42. Abramyan J. Hedgehog signaling and embryonic craniofacial disorders. *J Dev Biol*. 2019;7(2):1–26. doi:10.3390/jdb7020009
43. Zayzafoon M. Calcium/calmodulin signaling controls osteoblast growth and differentiation. *J Cell Biochem*. 2006;97(1):56-70. doi:10.1002/jcb.20675
44. Abzhanov A. Darwin's Finches: analysis of beak morphological changes during evolution. *Cold Spring Harb Protoc*. 2009;4(3):pdb.emo119. doi:10.1101/pdb.emo119
45. Hao Y, Tang S, Yuan Y, Liu R, Chen Q. Roles of FGF8 subfamily in embryogenesis and oral-maxillofacial diseases

(review). *Int J Oncol*. 2019;54(3):797-806. doi:10.3892/ijo.2019.4677
46. Chen H, Cui Y, Zhang D, Xie J, Zhou X. The role of fibroblast growth factor 8 in cartilage development and disease. *J Cell Mol Med*. 2022;26(4):990-999. doi:10.1111/jcmm.17174
47. Massague J. Integration of Smad and MAPK pathways: a link and a linker revisited. *Genes Dev*. 2003;17(24):2993-2997. doi:10.1101/gad.1167003
48. Estaras C, Benner C, Jones KA. SMADs and YAP compete to control elongation of beta-catenin:LEF-1-recruited RNAPII during hESC differentiation. *Mol Cell*. 2015;58(5):780-793. doi:10.1016/j.molcel.2015.04.001
49. Dituri F, Cossu C, Mancarella S, Giannelli G. The interactivity between TGFbeta and BMP signaling in organogenesis, fibrosis, and cancer. *Cells*. 2019;8(10):1130. doi:10.3390/cells8101130
50. Mourtada J, Thibaudeau C, Wasylyk B, Jung AC. The multi-faceted role of human dickkopf-3 (DKK-3) in development, immune modulation and cancer. *Cells*. 2023;13(1):75. doi:10.3390/cells13010075
51. Cooney RA, Saal ML, Geraci KP, et al. A WNT4- and DKK3-driven canonical to noncanonical WNT signaling switch controls multiciliogenesis. *J Cell Sci*. 2023;136(16):1–15. doi:10.1242/jcs.260807
52. Leonard JL, Leonard DM, Wolfe SA, et al. The Dkk3 gene encodes a vital intracellular regulator of cell proliferation. *PLoS One*. 2017;12(7):e0181724. https://doi.org10.1371/journal.pone.0181724
53. Itasaki N, Hoppler S. Crosstalk between Wnt and bone morphogenic protein signaling: a turbulent relationship. *Dev Dyn*. 2010;239(1):16-33. doi:10.1002/dvdy.22009
54. Lex RK, Vokes SA. Timing is everything: transcriptional repression is not the default mode for regulating hedgehog signaling. *Bioessays*. 2022;44(12):e2200139. doi:10.1002/bies.202200139
55. Attisano L, Wrana JL. Signal integration in TGF-beta, WNT, and hippo pathways. *F1000prime Rep*. 2013;5:17. doi:10.12703/P5-17
56. Mak SS, Wrabel A, Nagai H, Ladher RK, Sheng G. Zebra finch as a developmental model. *Genesis*. 2015;53(11):669-677. doi:10.1002/dvg.22900
57. Griffith SC, Buchanan KL. The zebra finch: the ultimate Australian supermodel. *Emu—Austral Ornithol*. 2016;110(3):v-xii. doi:10.1071/MUv110n3_ED
58. Karten HJ, Brzozowska-Prechtl A, Lovell PV, et al. Digital atlas of the zebra finch (*Taeniopygia guttata*) brain: a high-resolution photo atlas. *J Comp Neurol*. 2013;521(16):3702-3715. doi:10.1002/cne.23443
59. Poirier C, Vellema M, Verhoye M, et al. A three-dimensional MRI atlas of the zebra finch brain in stereotaxic coordinates. *Neuroimage*. 2008;41(1):1-6. doi:10.1016/j.neuroimage.2008.01.069
60. Warren WC, Clayton DF, Ellegren H, et al. The genome of a songbird. *Nature*. 2010;464(7289):757-762. doi:10.1038/nature08819
61. Murray JR, Varian-Ramos CW, Welch ZS, Saha MS. Embryological staging of the zebra finch, *Taeniopygia guttata*. *J Morphol*. 2013;274(10):1090-1110. doi:10.1002/jmor.20165
62. Badyaev AV. The beak of the other finch: coevolution of genetic covariance structure and developmental modularity during adaptive evolution. *Philos Trans R Soc B*. 2010;365:1111-1126.
63. Mallarino R, Grant PR, Grant BR, Herrel A, Kuo WP, Abzhanov A. Two developmental modules establish 3D beak-shape variation in Darwin's finches. *Proc Natl Acad Sci USA*. 2011;108(10):4057-4062. doi:10.1073/pnas.1011480108
64. Abzhanov A, Kuo WP, Hartmann C, Grant BR, Grant PR, Tabin CJ. The calmodulin pathway and evolution of elongated beak morphology in Darwin's finches. *Nature*. 2006;442(7102):563-567. doi:10.1038/nature04843
65. Schneider RA. How to tweak a beak: molecular techniques for studying the evolution of size and shape in Darwin's finches and other birds. *Bioessays*. 2007;29(1):1-6. doi:10.1002/bies.20517
66. Sánchez Moreno C, Badyaev AV. Transient epithelial mimicry reconciles stemness and regional specification in neural crest cells of avian beaks. *Evolution & Development*. 2026;28(2):e70044. doi:10.1101/2025.05.29.656909
67. Szabo-Rogers HL, Geetha-Loganathan P, Whiting CJ, Nimmagadda S, Fu K, Richman JM. Novel skeletogenic patterning roles for the olfactory pit. *Development*. 2009;136(2):219-229. doi:10.1242/dev.023978
68. Albawaneh Z, Ali R, Abramyan J. Novel insights into the development of the avian nasal cavity. *Anat Rec*. 2021;304(2):247-257. doi:10.1002/ar.24349
69. Jomaa J, Martinez-Vargas J, Essaili S, Haider N, Abramyan J. Disconnect between the developing eye and craniofacial prominences in the avian embryo. *Mech Dev*. 2020;161:103596. doi:10.1016/j.mod.2020.103596
70. Valenta T, Hausmann G, Basler K. The many faces and functions of beta-catenin. *EMBO J*. 2012;31(12):2714-2736. doi:10.1038/emboj.2012.150
71. Hyytiainen M, Penttinen C, Keski-Oja J. Latent TGF-beta binding proteins: extracellular matrix association and roles in TGF-beta activation. *Crit Rev Clin Lab Sci*. 2004;41(3):233-264. https://doi.org10.1080/10408360490460933
72. Sachan N, Phoon CKL, Bu L, Zilberberg L, Ahamed J, Rifkin DB. Binding requirements for latent transforming growth factor Beta2 activation. *Matrix Biol Plus*. 2024;22:100149. https://doi.org10.1016/j.mbplus.2024.100149
73. Badyaev AV, Lee CA, Gleason MJ, et al. Cell jamming transitions can affect regulatory protein gradients and prime evolutionary divergence. *J R Soc Interface*. 2025;22(232):20250186. doi:10.1098/rsif.2025.0186
74. Badyaev AV, Sánchez Moreno C, Lee CA, Britton SE, Johnstone LM, Duckworth RA. Ultimate paths of least resistance: intrinsically disordered proteins as developmental resets in regulatory networks. *Proc R Soc B*. 2025;292:20252393.
75. Mallarino R, Campas O, Fritz JA, et al. Closely related bird species demonstrate flexibility between beak morphology and underlying developmental programs. *Proc Natl Acad Sci USA*. 2012;109:16222-16227.
76. Keller B, Yang T, Chen Y, et al. Interaction of TGFbeta and BMP signaling pathways during chondrogenesis. *PLoS One*. 2011;6(1):e16421. doi:10.1371/journal.pone.0016421
77. Pathi S, Rutenberg JB, Johnson RL, Vortkamp A. Interaction of Ihh and BMP/noggin signaling during cartilage differentiation. *Dev Biol*. 1999;209:239-253.

78. Goodnough LH, Chang AT, Treloar C, Yang J, Scacheri PC, Atit RP. Twist1 mediates repression of chondrogenesis by beta-catenin to promote cranial bone progenitor specification. *Development*. 2012;139(23):4428-4438. doi:10.1242/dev.081679
79. Woronowicz KC, Schneider RA. Molecular and cellular mechanisms underlying the evolution of form and function in the amniote jaw. *Evodevo*. 2019;10:17. doi:10.1186/s13227-019-0131-8
80. Mak KK, Kronenberg HM, Chuang PT, Mackem S, Yang Y. Indian hedgehog signals independently of PTHrP to promote chondrocyte hypertrophy. *Development*. 2008;135(11):1947-1956. doi:10.1242/dev.018044
81. Deng A, Zhang H, Hu M, et al. The inhibitory roles of Ihh downregulation on chondrocyte growth and differentiation. *Exp Ther Med*. 2018;15(1):789-794. doi:10.3892/etm.2017.5458
82. Sun Q, Huang J, Tian J, et al. Key roles of Gli1 and Ihh signaling in craniofacial development. *Stem Cells Dev*. 2024;33(11–12):251-261. doi:10.1089/scd.2024.0036
83. Hill TP, Spater D, Taketo MM, Birchmeier W, Hartmann C. Canonical Wnt/beta-catenin signaling prevents osteoblasts from differentiating into chondrocytes. *Dev Cell*. 2005;8(5):727-738. doi:10.1016/j.devcel.2005.02.013
84. Day TF, Guo X, Garrett-Beal L, Yang Y. Wnt/beta-catenin signaling in mesenchymal progenitors controls osteoblast and chondrocyte differentiation during vertebrate skeletogenesis. *Dev Cell*. 2005;8(5):739-750. https://doi.org10.1016/j.devcel.2005.03.016
85. Yin H, Duan L, Wang Z, Liu L, Shen J. Fibroblast growth factor 8: multifaceted role in development and developmental disorder. *Genes Dis*. 2025;12(5):101524. doi:10.1016/j.gendis.2025.101524
86. Bryant DM, Stow JL. Nuclear translocation of cell-surface receptors: lessons from fibroblast growth factor. *Traffic*. 2005;6(10):947-954. doi:10.1111/j.1600-0854.2005.00332.x
87. Sánchez-Serna G, Badia-Ramentol J, Bujosa P, et al. Less, but more: new insights from Appendicularians on chordate Fgf evolution and the divergence of tunicate lifestyles. *Mol Biol Evol*. 2025;42(1):1–21. doi:10.1093/molbev/msae260
88. Suzuki A, Harada H, Nakamura H. Nuclear translocation of FGF8 and its implication to induce Sprouty2. *Dev Growth Differ*. 2012;54(4):463-473. doi:10.1111/j.1440-169X.2012.01332.x
89. Dash S, Trainor PA. Nucleolin loss-of-function leads to aberrant FGF signaling and craniofacial anomalies. *bioRxiv*. 2021;2021–09. doi:10.1101/2021.09.14.460382
90. Cheng Y, Lei F. Avian lower beak is always overlooked: its coordinate role in shaping species-specific beak should not be underestimated. *Integr Zool*. 2024;19(2):339-342. doi:10.1111/1749-4877.12769
91. Eames BF, Schneider RA. The genesis of cartilage size and shape during development and evolution. *Development*. 2008;135(23):3947-3958. doi:10.1242/dev.023309
92. Ealba EL, Jheon AH, Hall J, Curantz C, Butcher KD, Schneider RA. Neural crest-mediated bone resorption is a determinant of species-specific jaw length. *Dev Biol*. 2015;408(1):151-163. doi:10.1016/j.ydbio.2015.10.001
93. Dejana E, Hirschi KK, Simons M. The molecular basis of endothelial cell plasticity. *Nat Commun*. 2017;8:14361. doi:10.1038/ncomms14361
94. Asrar H, Tucker AS. Endothelial cells during craniofacial development: populating and patterning the head. *Front Bioeng Biotechnol*. 2022;10:962040. https://doi.org10.3389/fbioe.2022.962040
95. Galea GL, Zein MR, Allen S, Francis-West P. Making and shaping endochondral and intramembranous bones. *Dev Dyn*. 2021;250(3):414-449. doi:10.1002/dvdy.278
96. Percival CJ, Richtsmeier JT. Angiogenesis and intramembranous osteogenesis. *Dev Dyn*. 2013;242(8):909-922. doi:10.1002/dvdy.23992
97. Nemkov T, Kingsley PD, Dzieciatkowska M, et al. Circulating primitive murine erythroblasts undergo complex proteomic and metabolomic changes during terminal maturation. *Blood Adv*. 2022;6(10):3072-3089. doi:10.1182/bloodadvances.2021005975
98. Bruns GAP, Ingram VM. The erythroid cells and haemoglobins of the chick embryo. *Philos Trans R Soc B*. 1973;266:225-305.
99. Goldman DC, Bailey AS, Pfaffle DL, Al Masri A, Christian JL, Fleming WH. BMP4 regulates the hematopoietic stem cell niche. *Blood*. 2009;114(20):4393-4401. doi:10.1182/blood-2009-02-206433
100. Krimpenfort RA, Nethe M. Canonical Wnt: a safeguard and threat for erythropoiesis. *Blood Adv*. 2021;5(18):3726-3735. doi:10.1182/bloodadvances.2021004845
101. Guedes PT, de Oliveira BC, Manso PP, Caputo LF, Cotta-Pereira G, Pelajo-Machado M. Histological analyses demonstrate the temporary contribution of yolk sac, liver, and bone marrow to hematopoiesis during chicken development. *PLoS One*. 2014;9(3):e90975. doi:10.1371/journal.pone.0090975
102. Lee CA, Sanchez Moreno C, Badyaev AV. FInCH: Fiji plugin for automated and scalable whole-image analysis of protein expression and cell morphology. *MethodsX*. 2024;13:102855. doi:10.1016/j.mex.2024.102855

SUPPORTING INFORMATION

Additional supporting information can be found online in the Supporting Information section at the end of this article.

How to cite this article: Duckworth RA, Britton SE, Lee CA, Chenard KC, Badyaev AV. Spatial and temporal coordination of signaling pathways in tissue differentiation: Developmental atlas of protein expression during zebra finch beak maturation. *Developmental Dynamics*. 2026;1-26. doi:10.1002/dvdy.70156